Mechanical Systems and Signal Processing 68-69 (2016) 217–244

Contents lists available at ScienceDirect

Mechanical Systems and Signal Processing

journal homepage: www.elsevier.com/locate/ymssp

General framework for transfer path analysis: History, theory and classification of techniques ☆

Maarten V. van der Seijs [a,*], Dennis de Klerk [a,b], Daniel J. Rixen [c]

[a] Delft University of Technology, Faculty of Mechanical, Maritime and Material Engineering, Department of Precision and Microsystems Engineering, Section Engineering Dynamics, Mekelweg 2, 2628CD Delft, The Netherlands
[b] Müller-BBM VibroAkustik Systeme GmbH, Robert-Koch-Strasse 13, 82152 Planegg, Germany
[c] Technische Universität München, Faculty of Mechanical Engineering, Institute of Applied Mechanics, Boltzmannstr. 15, 85748 Garching, Germany

ARTICLE INFO

Article history:
Received 20 March 2015
Received in revised form
29 July 2015
Accepted 3 August 2015
Available online 28 August 2015

Keywords:
Transfer path analysis
Source characterisation
Vibration transmission
Dynamic substructuring

ABSTRACT

Transfer Path Analysis (TPA) designates the family of test-based methodologies to study the transmission of mechanical vibrations. Since the first adaptation of electric network analogies in the field of mechanical engineering a century ago, a multitude of TPA methods have emerged and found their way into industrial development processes. Nowadays the TPA paradigm is largely commercialised into out-of-the-box testing products, making it difficult to articulate the differences and underlying concepts that are paramount to understanding the vibration transmission problem. The aim of this paper is to derive and review a wide repertoire of TPA techniques from their conceptual basics, liberating them from their typical field of application. A selection of historical references is provided to align methodological developments with particular milestones in science. Eleven variants of TPA are derived from a unified framework and classified into three categories, namely classical, component-based and transmissibility-based TPA. Current challenges and practical aspects are discussed and reference is made to related fields of research.

1. Introduction

Transfer Path Analysis (TPA) has been a valuable engineering tool for as long as noise and vibrations of products have been of interest. A TPA concerns a product's actively vibrating components (such as engines, gearing systems or turbochargers) and the transmission of these vibrations to the connected passive structures. TPA is particularly useful when the actual vibrating mechanisms are too complex to model or measure directly, as it allows us to represent a source by forces and vibrations displayed at the interfaces with the passive side.

In this way the *source excitations* can be separated from the structural/acoustic *transfer characteristics*, allowing us to troubleshoot the dominant paths of vibration transmission. The engineer can then anticipate by making changes to either the source itself or the receiving structures that are connected to it.

☆ This research was funded and supported by the BMW Group.
* Corresponding author.
E-mail addresses: m.v.vanderseijs@tudelft.nl (M.V. van der Seijs), ddeklerk@muellerbbm-vas.nl (D. de Klerk), rixen@tum.de (D.J. Rixen).

http://dx.doi.org/10.1016/j.ymssp.2015.08.004

Nomenclature

DoF	degree of freedom
FRF	frequency response function
u	dynamic displacements/rotations
f	applied forces/moments
g	interface forces/moments
Y	admittance FRF matrix
Z	impedance FRF matrix
T	transmissibility matrix
$\star^{AB}$	pertaining to the assembled system
$\star^{A}$, $\star^{B}$	pertaining to the active/passive component
$\star^{R}$	pertaining to the test rig
$\star_1$	source excitation DoF
$\star_2$	interface DoF
$\star_3$	receiver DoF
$\star_4$	indicator DoF
$\star_{ps}$	pseudo-force DoF

A TPA often rises from the need to reduce some sort of undesired noise or vibration, for instance to improve product comfort or lifetime, ensure safety or preserve stealthiness. Aside from automotive development, applications are also seen in industries such as marine and aeroplane engineering, building acoustics and acoustic modelling of musical instruments. A TPA is generally motivated by one of the following desires:

1. *Secrecy*: perhaps the earliest TPA studies were triggered by the need to reduce the transmission of engine vibrations in military ships and submarines in order to make them stealthy. Many publications in the 1950s and 1960s document on isolation of ship engines by means of absorbers and decoupling mechanisms [1–5] to minimise the transmission through the interfaces.
2. *Safety*: along with the rapid development of aeroplanes and spacecraft in the 1960s, TPA concepts started to be of use to study fatigue and stability (flutter) problems due to active or induced vibrations. As sources of vibrations are much more persistent in aeronautics – think of vortex-induced vibrations – focus was on characterising the passive transfer paths by means of modal analysis [6,7].
3. *Comfort*: over the last decades TPA tends to be particularly associated with noise, vibration and harshness (NVH) engineering as commonly encountered in the automotive industry. The majority of recent developments and commercial solutions have been tailored towards this engineering society or related industries, driven by the increasing customer expectations on acoustic comfort [8–12].

In response to the evolving demands, TPA methods have been under continuous development and their family members have grown numerous. Some designations that found their way into the literature include Operational TPA (OTPA), Operational Path Analysis with exogenous inputs (OPAX), blocked-force TPA, Gear Noise Propagation, in situ Source Path Characterisation and Virtual Acoustic Prototyping. Very often those methods are presented from highly case-specific derivations. Not surprisingly, as the underlying physical concepts are similar, some of the above-mentioned show strong similarities or are even identical.

A TPA work flow can typically be subdivided in the following steps: (a) operational measurement on the active component; (b) determination of the passive (sub)system characteristics (commonly by means of FRFs); (c) identification of interface loads; (d) calculation of path contributions. The steps are shown schematically in Fig. 1. Depending on the TPA method at hand, some or all of these steps may be performed in arbitrary order. The optimisation actions that follow from such an analysis are generally not considered part of the work flow.

This paper presents a unified framework for derivation of a large range of TPA methods. It is chosen to present and classify the methods separate from their typical fields of application, such that the underlying physical concepts are exposed and can be compared. Section 2 presents an account of some early developments and their relation to currently established TPA methods. This should by no means be regarded as a complete historical overview; rather it was chosen to highlight some key publications that have inspired the methodological developments in different ways. In Section 3 a general framework for TPA is introduced, starting by depicting the transfer problem using the Dynamic Substructuring paradigm [13]. Hereafter the TPA methods are derived and classified along three families, namely the *classical* (Section 3.2), *component-based* (Section 3.3) and *transmissibility-based* (Section 3.4) TPA methods, as depicted vertically in Fig. 1.

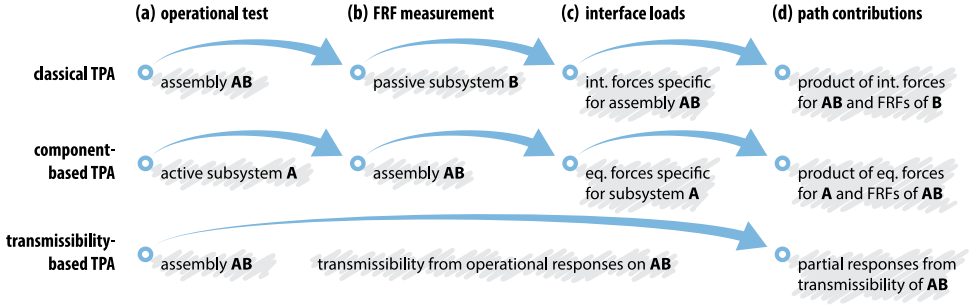

Fig. 1. The TPA work flow, depicted stepwise for the three TPA families.

The paper is concluded in Section 4 with a discussion of some practical aspects that are more common to TPA and partly application-specific.

2. Historical overview

Transfer Path Analysis has been developed mostly during the second half of the 20th century, although some fundamental concepts date back to the 1880s. As often occurs in science, inspiration was found in different fields of research. This section starts with describing the adaptation of linear electric network theory to describe the transfer of structural vibrations. These form the foundations on which many analytical, and later also experimental TPA techniques have been built.

2.1. Impedance and mobility concepts

The inherent task of analysing a transfer problem is to describe the relation between the inputs and outputs of systems, preferably in a systematic or lumped way. Some of the major contributions in system theory originate from electric network science, founded on the laws for electric circuits of Kirchhoff [14], the superposition principle and the definitions of electric quantities such as admittance and impedance by Heaviside [15]. The equivalent source theorems of Thévenin [16] and Norton [17] were stated[1] by the turn of the 20th century, allowing us to substitute a group of active and passive components by an equivalent voltage/current and a single impedance. Altogether these discoveries provided a handful of tools to depict complex electrical systems as a set of lumped subsystems, characterised by frequency dependent properties (e.g. impedance, admittance) and interacting by the so-called “through” and “across” quantities, e.g. current and voltage.

The electric network principles appeared equally useful to describe structural vibrations of mechanical systems. Gardonio and Brennan published an extensive review [21] of the system description based on impedance and mobility (admittance) concepts in structural dynamics. They regard the article of Webster in 1914 [22] as the first effort to demonstrate analogies between electrical and mechanical impedance properties. In an attempt to describe the acoustic pressure in horns and musical instruments, Webster defined the acoustical impedance as the complex frequency-dependent ratio between pressure and volume of flowing air. From thereon analogies have been derived for mechanical systems,[2], which is thoroughly reviewed in [21,25].

Impedance and mobility have since been well established as concepts to model and understand all sorts of vibratory systems [26–29]. The adaptation of the four-pole matrix method [30] furthermore introduced means to model systems consisting of a larger sequence of subsystems. However, most applications remained limited to fairly analytic cases [2–4]. In particular, the topic of experimental source characterisation has received little attention until the 1970s.

2.2. Advancing experimental techniques

Between 1971 and 1981 Bendat and Piersol provided a comprehensive set of spectral correlation and coherence functions with special attention for digital data acquisition [31–34]. These publications have empowered multiple-input/multiple-output (MIMO) measurement techniques that are instrumental to many advanced analyses, such as multi-reference modal testing [35]. Indeed the engineers were now given the chance to analyse vibration problems in their full complexity (e.g. multi-path, multi-DoF) rather than by simplified or analytical descriptions.

During the decades that followed, various simultaneous developments have been observed that led to a rapid expansion of practical TPA methods:

- The first exploration of techniques nowadays denoted as *classical TPA* is often attributed to the work of Verheij around 1980 who studied the transmission of ship machinery vibrations through resilient mounts [36,37]. Although theory on mount stiffness had been around already for years [5], Verheij was one of the first to successfully determine interface forces and moments by experiment. Although attractive from an academical point of view, practical engineering called for less elaborate force determination methods. The matrix-inverse technique proved to be a good alternative [38–41] and is up to today one of the most popular classical TPA methods in practice. The theory of classical TPA is presented in Section 3.2.
- In 1981 Magrans proposed a general method of measuring transmissibility between terminals in a network [42]. The so-called Global Transfer Direct Transfer (GTDT) method was further explored by Guasch [43–45] and later put into practice as the Advanced TPA [46]. Independently, Liu and Ewins [47] and Varoto and McConnell [48] explored properties of transmissibility matrices for structural vibrational problems, followed up by Ribeiro, Maia, Silva and Fontul [49–52]. Surprisingly though, the transmissibility-based method known as *Operational TPA* was first presented (again

[1] Actually it was Helmholtz who posed the equivalent source theorem already in 1853 in one of his fundamental works [18]. Like many scientist in that time, Thévenin was not aware of this early finding, as can be read in [19,20].

[2] The initial analogy regarded force analogous to voltage, which seemed the most intuitive choice. Firestone however disqualified this mechanical-impedance analogy in 1933 [23], arguing that it infringes Kirchhoff's definitions of the terms *through* and *across*. The mechanical-mobility analogy, linking force with electrical current, is indeed the correct analogy for drawing mechanical circuits using parallel and series addition [24]. Nevertheless, the terms impedance and mobility have never changed definition in common use.

independently) by Noumura and Yoshida in Japan [53]. Section 3.4 discusses the theory and related techniques; reviews and benchmark studies are found in [54–57].

- Inspired on acoustics, Mondot and Petersson proposed a method in 1987 to depict the vibration transfer problem using the characteristic power of the source itself (the so-called source descriptor) and a coupling function accounting for the added dynamics of the receiving structure [58]. This triggered the idea to characterise a source by means of blocked forces or free velocities [59–61], as seen in e.g. the *in situ* method by Moorhouse and Elliott [62,63] and the *pseudo-forces* method by Janssens and Verheij [64,65]. These and other strategies based on source component description are discussed in Section 3.3.
- Most TPA methods require admittance of either the source, receiver or assembled structure. Dynamic Substructuring (DS) techniques are particularly useful for this purpose, as they allow us to assemble systems from the dynamics of its substructures [13]. Component Mode Synthesis (CMS) and model reduction [66–68] emerged in the 1960s as the first application of DS. Rather than characterising an input/output problem, their main purpose was to compute natural modes and frequencies of aerospace structures. This perhaps explains why DS techniques were hardly ever brought in context with TPA.[3] Yet with the introduction of Frequency Based Substructuring (FBS) [72,73] in the late 1980s, methods became available to assemble multiple substructures from FRFs, either obtained from numerical modelling or admittance tests [74]. In fact, DS theory appeared very convenient to derive hybrid numerical/experimental TPA schemes and perform component optimisation [75,76]. This is particularly effective in combination with component-based TPA schemes [77,78], as discussed in Section 3.3.

2.3. Towards general TPA methodologies

The abundance of developments brought prosperity to the engineering community, yet at the same time raised misunderstanding about the interrelations between the methods. In 1980 the ISO work group TC43/SC1/WG22 was established, dedicated to investigating and standardising the present technologies for structure-borne TPA [79,80]. An intermediate report [81] already presented a comprehensive overview, addressing aspects such as the required number of DoFs, source description by means of equivalent quantities (forces/velocities/power), reciprocal measurement techniques and potential integration of Statistical Energy Analysis (SEA) principles. Although well accepted by acoustical engineers, the standardisations failed to gain broad popularity in the field of structure-borne TPA.

Nevertheless, popular methods such as operational TPA and matrix-inverse TPA have nowadays been integrated into many commercial noise and vibration solutions. Extensive literature is currently available, often discussing the application of a particular technique in a case-specific fashion. From such perspective the relation with other TPA techniques can be vague. In the remaining of this paper it is attempted to review the landscape of TPA techniques in a unified way, namely from the framework as presented next.

3. Framework for transfer path analysis

The framework for Transfer Path Analysis as presented here follows the notation and terminology of Frequency Based Substructuring (FBS) [13]. Although different styles of derivation are encountered in the literature, it is the authors' belief that the transfer path problem is best understood by describing the dynamic interaction between the active and passive subsystems.

In Section 3.1 the subsystem definition is introduced and the transfer problem is formulated based on the admittances[4] of the active and passive subsystems. Thereafter a distinction is made between three families of TPA methods, respectively denoted as *classical TPA* (Section 3.2), *component-based TPA* (Section 3.3) and *transmissibility-based TPA* (Section 3.4). A summary is presented in Section 3.5.

3.1. The transfer path problem

Let us consider the dynamic system AB as schematically depicted in Fig. 2a. Two subsystems can be distinguished: an active subsystem A containing an excitation at node 1 and a passive subsystem B comprising the responses of interest at node 3. The subsystems are rigidly interconnected at the interface node 2. For simplicity of derivation, the Degrees of Freedom (DoFs) in this example are restricted to three distinct nodes. These may however represent a larger set of DoFs, representing respectively

1. *source*: internal DoFs belonging to the active component that cause the operational excitation but are unmeasurable in practice;
2. *interface*: coupling DoFs residing on the interface between the active and the passive component;
3. *receiver*: response DoFs at locations of interest at the passive component, possibly including acoustic pressures and other physical quantities.

[3] Early examples that suggest relations between TPA and dynamic substructuring are papers of Rubin [69,70] (who later published an important modal reduction method [71]) and a NASA report [7].

[4] Dynamic systems can be characterised and assembled using either impedance or admittance notations [27–29,82]. As admittances are obtained more naturally in experimental practice, they are favoured throughout the derivations.

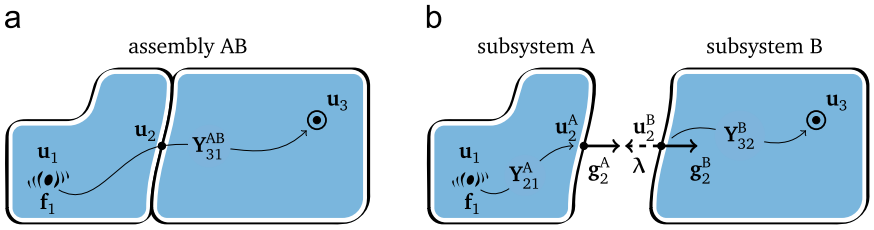

Fig. 2. The transfer path problem: (a) based on the admittance of assembly AB and (b) based on the admittances of subsystems A and B.

Hence, the example of Fig. 2a is illustrative for a wide range of practical problems, provided that the structure of interest can be decomposed into an active and a passive part. In what follows, all methods assume that the operational excitation at node 1 is unmeasurable in practice, but transmits vibrations through the interfaces at node 2 to receiving locations at node 3. The responses shall then be built up from a certain description of the vibrations measured at the interface (node 1→2) and an appropriate set of transfer functions relating these vibrations to the receiving responses (node 2→3). The fundamental choices herein dictate to which TPA family the method is classified.

3.1.1. *Transfer path from assembled admittance*

Let us first approach the transfer problem top-down for the assembled system AB, see Fig. 2a. We are interested in the response spectra at the receiving locations $\mathbf{u}_3(\omega)$ for source excitations at node 1, given by the force spectra $\mathbf{f}_1(\omega)$. For the assembled problem, this is simply obtained from a superposition of the individual contributions, i.e. the excitation force spectra multiplied with their respective linear(ised) transfer functions, contained in the columns of admittance FRF matrix $\mathbf{Y}^{AB}(\omega)$

$$u_i(\omega) = \sum_j Y_{ij}^{AB}(\omega) f_j(\omega) \implies \mathbf{u}_3(\omega) = \mathbf{Y}_{31}^{AB}(\omega)\,\mathbf{f}_1(\omega) \tag{1}$$

In the equations that follow the explicit frequency dependency (ω) will be omitted to improve readability. Also note that the response set $\mathbf{u}$ can include displacements, velocities, accelerations or any other quantity, provided that the rows of the FRF matrices are obtained accordingly. Furthermore, in order to keep the derivations brief and understandable, it is chosen to only consider the structure-borne paths. Nevertheless, Eq. (1) can easily be extended to include contributions of airborne paths if the application so requires. In that case $\mathbf{Y}$ and $\mathbf{f}$ need to be augmented with a set of (responses to) acoustic loads such as volume velocities (m^3/s), as further discussed in Section 4.3.

3.1.2. *Transfer path from subsystem admittance*

The same transfer function is now derived for an assembly of the individual subsystems, as depicted in Fig. 2b. Let us first put the subsystem's FRF matrices $\mathbf{Y}^A$ and $\mathbf{Y}^B$ in a block-diagonal format. The force vector comprising the excitation force is augmented with interface forces $\mathbf{g}_2$ for both sides of node 2 that are yet to be determined. The obtained system of equations resembles the admittance variant of dual assembly, which is a standard form of Dynamic Substructuring [13]

$$\begin{bmatrix} \mathbf{u}_1 \\ \mathbf{u}_2^A \\ \mathbf{u}_2^B \\ \mathbf{u}_3 \end{bmatrix} = \begin{bmatrix} \mathbf{Y}_{11}^A & \mathbf{Y}_{12}^A & \mathbf{0} & \mathbf{0} \\ \mathbf{Y}_{21}^A & \mathbf{Y}_{22}^A & \mathbf{0} & \mathbf{0} \\ \mathbf{0} & \mathbf{0} & \mathbf{Y}_{22}^B & \mathbf{Y}_{23}^B \\ \mathbf{0} & \mathbf{0} & \mathbf{Y}_{32}^B & \mathbf{Y}_{33}^B \end{bmatrix} \left(\begin{bmatrix} \mathbf{f}_1 \\ \mathbf{0} \\ \mathbf{0} \\ \mathbf{0} \end{bmatrix} + \begin{bmatrix} \mathbf{0} \\ \mathbf{g}_2^A \\ \mathbf{g}_2^B \\ \mathbf{0} \end{bmatrix} \right) \quad \text{or} \quad \mathbf{u} = \mathbf{Y}(\mathbf{f}+\mathbf{g}) \tag{2}$$

The following physical explanation can now be reasoned to solve Eq. (2). The excitation force at node 1 induces a motion at node 2 of subsystem A. As subsystem B is not directly affected by forces at A (due to the block-diagonal form of the global FRF matrix), an incompatibility is caused between $\mathbf{u}_2^A$ and $\mathbf{u}_2^B$. This is denoted by the interface "gap" $\boldsymbol{\delta}$, which can conveniently be written using a signed Boolean matrix[5] $\mathbf{B}$ as shown in Eqs. (3a) and (3c). Next, assuming that no additional mass is present between the subsystems, the *equilibrium condition* is satisfied, requiring the interface forces $\mathbf{g}_2$ on both sides to be equal in magnitude and opposing in sign. The interface forces are expressed by Eqs. (3b) and (3c), using a Lagrange multiplier $\boldsymbol{\lambda}$ for the magnitude and the transposed Boolean matrix to account for the interface force direction

$$\boldsymbol{\delta} = \mathbf{u}_2^B - \mathbf{u}_2^A \quad \text{or} \quad \boldsymbol{\delta} \triangleq \mathbf{B}\mathbf{u} \tag{3a}$$

$$\mathbf{g}_2^A = -\mathbf{g}_2^B = \boldsymbol{\lambda} \quad \text{or} \quad \mathbf{g} \triangleq -\mathbf{B}^T\boldsymbol{\lambda} \tag{3b}$$

$$\text{with } \mathbf{B} = \begin{bmatrix} \mathbf{0} & -\mathbf{I} & \mathbf{I} & \mathbf{0} \end{bmatrix} \tag{3c}$$

The interface forces $\boldsymbol{\lambda}$ that pull the two subsystems together can be determined from Eq. (3a) by requiring $\boldsymbol{\delta}=\mathbf{0}$, which enforces the *compatibility condition* $\mathbf{u}_2^A = \mathbf{u}_2^B$. Considering Eq. (3b), the interface forces that ensure compatibility can be

[5] The signed Boolean matrix $\mathbf{B}$ establishes the relations for all interface DoFs of A and B that are vectorially associated, e.g. u_{2x}^A and u_{2x}^B. Guidelines on the construction and properties of the signed Boolean matrix are found in [13].

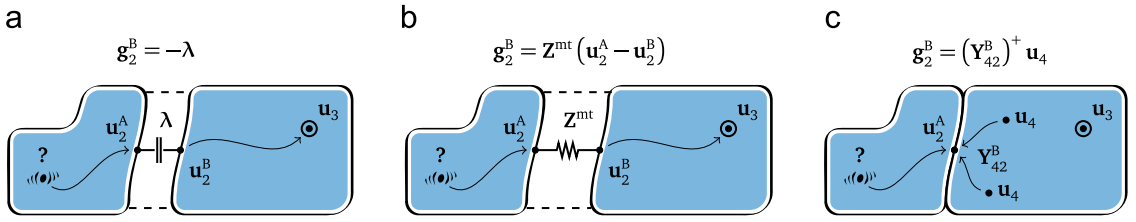

Fig. 3. Three approaches to determine the operational interface forces in classic TPA. (a) Direct force. (b) Mount stiffness. (c) Matrix inverse.

determined by equating the second and the third line of Eq. (2) and solving for $\boldsymbol{\lambda}$

$$\begin{aligned} \mathbf{Y}_{21}^A\mathbf{f}_1 + \mathbf{Y}_{22}^A\mathbf{g}_2^A &= \mathbf{Y}_{22}^B\mathbf{g}_2^B \\ \left(\mathbf{Y}_{22}^A + \mathbf{Y}_{22}^B\right)\boldsymbol{\lambda} &= -\mathbf{Y}_{21}^A\mathbf{f}_1 \\ \boldsymbol{\lambda} &= -(\mathbf{Y}_{22}^A + \mathbf{Y}_{22}^B)^{-1}\mathbf{Y}_{21}^A\mathbf{f}_1 \quad \Rightarrow \quad \mathbf{g}_2^B = (\mathbf{Y}_{22}^A + \mathbf{Y}_{22}^B)^{-1}\mathbf{Y}_{21}^A\mathbf{f}_1 \end{aligned} \tag{4}$$

Eq. (4) provides the interface forces at the coinciding interface DoFs caused by the operational excitation $\mathbf{f}_1$ inside subsystem A. The response at the receiving side $\mathbf{u}_3^B$ is found by substituting Eq. (4) into the last line of Eq. (2)

$$\mathbf{u}_3 = \mathbf{Y}_{32}^B\mathbf{g}_2^B = \underbrace{\left[\mathbf{Y}_{32}^B(\mathbf{Y}_{22}^A + \mathbf{Y}_{22}^B)^{-1}\mathbf{Y}_{21}^A\right]}_{\mathbf{Y}_{31}^{AB}}\mathbf{f}_1 \tag{5}$$

Comparing with Eq. (1), it follows that the terms between the brackets indeed represent the admittance of the assembly $\mathbf{Y}_{31}^{AB}$ by coupling of the subsystems' admittances. It can be verified that this result is in accordance with Lagrange Multiplier Frequency Based Substructuring (LM-FBS) assembly [13], which is further elaborated in Appendix A.

So far it has been assumed that the excitation at node 1 is measurable. In reality however it is impossible or impractical to identify the exact force loading. This is solved in TPA by assuming that the dynamics at the interface node 2 due to this excitation are measurable and may very well represent the source excitation. In what follows, different approaches are examined to describe the transmission of vibrations, or rather, the response at the passive subsystem B for a non-measurable excitation somewhere inside (or on) the active subsystem A. The notation of Dynamic Substructuring is used to reveal the relations between different approaches.

3.2. Classical TPA

The family of *Classical TPA* methods is essentially intended to identify transfer path contributions in *existing products*. They have nowadays become standard practice to troubleshoot NVH problems in automotive engineering [9,10]. A classical TPA performs operational tests on the assembled product AB to obtain interface forces between the active and the passive side, namely $\boldsymbol{\lambda}$ in Eq. (4). It can be verified from Eqs. (2) and (5) that these interface forces fully determine the responses at the passive side and are thus representative for the effects of the source vibrations at the receiver locations $\mathbf{u}_3$. To calculate the receiver responses,[6] the passive-side interface forces $\mathbf{g}_2^B = -\boldsymbol{\lambda}$ are applied to the interfaces of subsystem B, as shown in Fig. 4a

$$\mathbf{u}_3 = \mathbf{Y}_{32}^B\mathbf{g}_2^B \tag{6}$$

Both steps pose some challenges in practice. The FRFs of the passive side are typically determined from impact or shaker tests, or in a reciprocal fashion using for instance an acoustic source at the receiving location and accelerometers at the interface nodes [83–87]. Either way it requires *dismounting* of the active part(s) from the passive side. With respect to the determination of operational interface forces $\mathbf{g}_2^B$, it could be impractical to mount force sensors between the active and the passive part. Therefore a number of indirect methods have been developed to circumvent direct force measurement.

Hence, the variants of classical TPA are defined according to how $\mathbf{g}_2^B$ is obtained from operational tests, which are discussed next.

3.2.1. Classical TPA: direct force

The most straightforward technique to obtain the interface forces is from force transducers mounted directly between the active and the passive side, as depicted in Fig. 3a. It was demonstrated by Eq. (4) that the interface force caused by the operational excitation is given by

$$\boldsymbol{\lambda} = -(\mathbf{Y}_{22}^A + \mathbf{Y}_{22}^B)^{-1}\mathbf{Y}_{21}^A\,\mathbf{f}_1 \quad \Longrightarrow \quad \mathbf{g}_2^B = -\boldsymbol{\lambda} \tag{7}$$

This is valid under the assumption that $\mathbf{u}_2^B = \mathbf{u}_2^A$, which requires the stiffness of the transducers to be high enough (relative to the stiffness of the actual subsystems) in the frequency range of interest. In fact, the main drawback of the method is the

[6] In this framework the resulting responses $\mathbf{u}_3$ are formulated as a matrix–vector product, namely the sum of the partial responses. Techniques to evaluate the individual transfer paths contributions are discussed in Section 4.5.

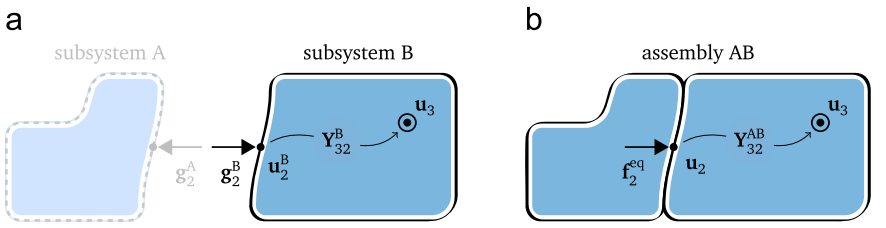

Fig. 4. Application of forces representing the operational excitation: classical TPA and component-based TPA. (a) Classic TPA: application of interface forces (measured under operation of assembled system AB) to the passive subsystem B. (b) Component-based TPA: application of equivalent forces (measured under operation of subsystem A) to the assembled system AB.

inconvenience of placing the transducers between the active component and the receiving structure. Lack of space, distortion of the original mounting situation and the incapability to measure all desired degrees of freedom at a connection point render the method impractical, especially for typical automotive applications. In case of large-scale systems such as ship machinery, this method may still be preferred [37].

3.2.2. Classical TPA: mount stiffness

An effective way of reducing vibration transmission is by placing resilient mounts between the components instead of rigid fixtures, as illustrated in Fig. 3b. By proper tuning of the mount flexibility (stiffness) and absorption (damping) properties, a high level of vibration suppression can be achieved. The mount stiffness method uses these mount properties to determine the interface forces. Assumed that the added mass of the mounts is negligible, the interface force equilibrium condition Eq. (3b) is still satisfied. However, the compatibility condition of Eq. (3a) is "weakened", hence $\mathbf{u}^{B}_{2}-\mathbf{u}^{A}_{2}$ is no longer zero. Instead the m interface forces and coordinate incompatibilities are related by the dynamic stiffnesses of the mounts, denoted by z^{mt}_{jj}, j representing a single interface DoF

$$\begin{bmatrix} g^{A}_{j} \\ g^{B}_{j} \end{bmatrix} = -z^{mt}_{jj}\begin{bmatrix} 1 & -1 \\ -1 & 1 \end{bmatrix}\begin{bmatrix} u^{A}_{j} \\ u^{B}_{j} \end{bmatrix} \Longrightarrow g^{B}_{j} = z^{mt}_{jj}(u^{A}_{j}-u^{B}_{j}), \quad j \in 1,\ldots,m$$

A spring-like stiffness matrix can be recognised, however with a minus sign because the interface forces g_j act on the connected subsystems A and B instead of the mount. Introducing the diagonal mount stiffness matrix $\mathbf{Z}^{mt}$, the full set of m interface forces $\mathbf{g}^{B}_{2}$ can be estimated from the differential interface displacements between the source and the receiver side, i.e. the measured displacements at both sides of the mounts

$$\mathbf{g}^{B}_{2} = \mathbf{Z}^{mt}(\mathbf{u}^{A}_{2}-\mathbf{u}^{B}_{2}) \quad \text{with } \mathbf{Z}^{mt} = \text{diag}(z^{mt}_{11}\ldots z^{mt}_{mm}) \tag{8}$$

In most cases the flexible mounts are already integrated in the design to attenuate the vibration transmission. If they are however placed in the system for the mere purpose of TPA, it can be shown that the interface forces and thus the vibrations of the coupled system are altered significantly [88,89], namely

$$\mathbf{g}^{B}_{2} = (\mathbf{Y}^{A}_{22}+\mathbf{Y}^{B}_{22}+\mathbf{Y}^{mt})^{-1}\mathbf{Y}^{A}_{21}\mathbf{f}_{1} \quad \text{with } \mathbf{Y}^{mt} = (\mathbf{Z}^{mt})^{-1}$$

Although the mount stiffness method can be powerful and easy to conduct, the accuracy is highly subject to the terms[7] in $\mathbf{Z}^{mt}$. Typical absorbers exhibit amplitude-dependent non-linearities and directional characteristics [1,2,91]. An advanced TPA method that estimates the mount properties from operational tests is discussed in Section 3.4.3.

3.2.3. Classical TPA: matrix inverse

The third and perhaps most popular classical TPA member is the matrix-inverse method [38–41]. It was observed from Eq. (6) that responses at the passive side are found from the application of the interface forces to the passive subsystem's FRFs. Recalling these responses from Eq. (2)

$$\begin{bmatrix} \mathbf{u}^{B}_{2} \\ \mathbf{u}_{3} \end{bmatrix} = \begin{bmatrix} \mathbf{Y}^{B}_{22} \\ \mathbf{Y}^{B}_{32} \end{bmatrix}\mathbf{g}^{B}_{2}$$

This problem can be inverted if the left-hand side contains sufficient independent responses to describe all m interface forces and moments in $\mathbf{g}^{B}_{2}$. The set of receiver responses $\mathbf{u}_3$ is typically too small in number and too distant from the interfaces to be suitable for inversion. Inversion of the first row is theoretically sufficient, but requires complete instrumentation of the assembled structure's interfaces to measure all DoFs $\mathbf{u}^{B}_{2}$ associated with $\mathbf{g}^{B}_{2}$. In addition, a symmetric FRF matrix $\mathbf{Y}^{B}_{22}$ would be required for the passive subsystem's interfaces, which is challenging to obtain accurately.[8]

[7] Note that the terms in the dynamic stiffness matrix $\mathbf{Z}^{mt}$ correspond to differential displacements of the associated interface DoFs $\mathbf{u}^{A}_{2}-\mathbf{u}^{B}_{2}$ and not the coordinates of both A and B. Some implications for the terms in $\mathbf{Z}^{mt}$ are discussed in [89,90].

[8] See Section 4.4 for a discussion on obtaining a full and reciprocal set of translational and rotational DoFs.

In practice, the passive side is equipped with the so-called *indicator responses* $\mathbf{u}_4$ as shown in Fig. 3c. An amount of $n \geq m$ responses shall be located in the proximity of the interfaces, such that the full set of m interface forces is properly *observable* from these points (this is addressed below). As these indicator DoFs merely assist in the determination of the interface forces, the sensor type can be chosen rather arbitrarily, although (tri-axial) accelerometers are the most common choice.

Two sets of measurements are now required to reconstruct the interface force spectra. First, responses $\mathbf{u}_4$ are measured on the assembled system AB during operational tests. These can be expressed in terms of subsystem admittances, similar to Eq. (5) (see also Appendix A)

$$\mathbf{u}_4 = \mathbf{Y}_{41}^{AB}\mathbf{f}_1 = \mathbf{Y}_{42}^{B}\underbrace{\left(\mathbf{Y}_{22}^{A}+\mathbf{Y}_{22}^{B}\right)^{-1}\mathbf{Y}_{21}^{A}\mathbf{f}_1}_{\mathbf{g}_2^B} \tag{9}$$

Next, FRFs need to be measured for the passive subsystem B, relating the motion at these indicator points to forces at the interface, namely $\mathbf{Y}_{42}^{B}$. Note that this requires dismounting of the active components from the assembly. Nevertheless, the FRFs $\mathbf{Y}_{42}^{B}$ (needed for the matrix-inverse force determination) and $\mathbf{Y}_{32}^{B}$ (to calculate responses at the target locations, Eq. (6)) can be obtained from the same FRF measurement campaign, as it only involves mounting of additional sensors. The operational interface forces can be reconstructed from a pseudo-inverse of the indicator response spectra $\mathbf{u}_4$ with the subsystem FRFs

$$\mathbf{g}_2^B = \left(\mathbf{Y}_{42}^{B}\right)^{+}\mathbf{u}_4 \tag{10}$$

If $\mathbf{Y}_{42}^{B}$ is full rank, it holds that $(\mathbf{Y}_{42}^{B})^{+}\mathbf{Y}_{42}^{B} = \mathbf{I}$, such that in theory the correct interface forces from Eq. (4) are obtained by subsequent application of Eqs. (9) and (10). Hence the conditioning of the FRF matrix is crucial, which should have (a) sufficient rank to describe all interface forces $\mathbf{g}_2^B$ independently from the set $\mathbf{u}_4$ and (b) a reasonably low condition number in order not to amplify measurement errors in the inversion. As a rule of thumb, it is common to use at least twice as many response DoFs as strictly required to fully determine the interface forces. Much attention has been devoted to improving the conditioning of the inverse problem by means of singular value decomposition, see for instance the work of Thite and Dobson [39–41,92,93] or an early review of techniques [94]. Time domain implementations have also been developed, such as the inverse structural filtering methods described in [38,95].

Recently there has been interest in the application of strain gages instead of the commonly used accelerometers at the indicator points. It is argued that strain responses possess a more direct relation to interface forces and are better able to capture the local phenomena of the structure. Consequently it is expected that strain measurements lead to better conditioning of the matrix to be inverted [96,97]. More research is currently needed to further verify this assumption.

3.3. Component-based TPA

A fundamentally different class of methods is that of the *component-based TPA*. As shown in Eq. (7), the interface forces obtained from a classical TPA are not a characteristic of the source alone but of the assembled dynamics. For that reason, a classical TPA cannot predict the effects of subsystem modification, as one would need to conduct a new operational test for every change in design. Hence, the interface forces measured in an assembly AB are not transferable to an assembly with another receiving side B.

Component-based TPA tries to characterise the source excitation by a set of equivalent forces or velocities that are an inherent property of the active component itself. The responses at the receiving side can be simulated by applying these forces to the FRFs of an assembled system with the active part shut down, as illustrated in Fig. 4b. Hence, the dynamic interaction with the passive side is accounted for in a later stage, at least not during operational measurements. This allows defining a testing environment[9] that is ideal for operational measurement on the active component, explaining the denotation *component-based*.

Interestingly, with respect to the origin of component-based TPA theory, literature has been very unambiguous. As mentioned in Section 2, some researchers have found inspiration in acoustics or electronic network theory (particularly the equivalent source identities of Thévenin and Norton), such as [58–63,98]. Others derived similar theories from a structural–mechanical point of view [64,65,99] or dynamic substructuring techniques [77,78]. As a consequence, a wide variety of component-based TPA methods have been derived, largely independent of each other. This section presents a more generic derivation in order to unite all component methods and compare the various concepts.

3.3.1. The equivalent source concept

Approaching the problem top-down, one is looking for a set of equivalent forces $\mathbf{f}_2^{eq}$ that, applied to the interface of the assembled system AB at rest, yields the correct responses at $\mathbf{u}_3$. This can be directly formulated using the admittance of the assembly $\mathbf{Y}_{32}^{AB}$, or expanded in terms of its subsystem admittances (see Appendix A)

$$\mathbf{u}_3 = \mathbf{Y}_{32}^{AB}\mathbf{f}_2^{eq} = \left[\mathbf{Y}_{32}^{B}\left(\mathbf{Y}_{22}^{A}+\mathbf{Y}_{22}^{B}\right)^{-1}\mathbf{Y}_{22}^{A}\right]\mathbf{f}_2^{eq} \tag{11}$$

[9] The dependency of the source excitation on the mounting conditions is discussed in Section 4.1.

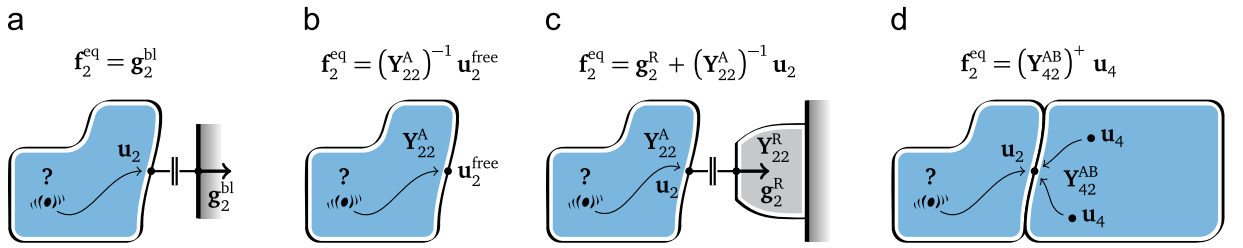

Fig. 5. Component-based TPA methods: various approaches to obtain equivalent forces representing the excitation. (a) Blocked force. (b) Free velocity. (c) Hybrid interface on test rig. (d) in situ in original assembly.

The response $\mathbf{u}_3$, as a result of the equivalent forces, should equal the response obtained when the active component is running in the same assembly, caused by $\mathbf{f}_1$ in Eq. (5). Comparing Eqs. (11) with (5), it follows naturally that the equivalent forces should take the form

$$\mathbf{Y}_{32}^{B}\left(\mathbf{Y}_{22}^{A}+\mathbf{Y}_{22}^{B}\right)^{-1}\mathbf{Y}_{22}^{A}\mathbf{f}_2^{eq} = \mathbf{Y}_{32}^{B}\left(\mathbf{Y}_{22}^{A}+\mathbf{Y}_{22}^{B}\right)^{-1}\mathbf{Y}_{21}^{A}\mathbf{f}_1 \quad\Longrightarrow\quad \mathbf{f}_2^{eq} = \left(\mathbf{Y}_{22}^{A}\right)^{-1}\mathbf{Y}_{21}^{A}\mathbf{f}_1 \tag{12}$$

Eq. (12) shows that the equivalent forces are indeed a property on the active component A only. The existence of such an equivalent source problem offers tremendous potential for practical component-based TPA methods. There is however one important limitation: *the equivalent forces only properly represent the operational excitations for responses on the receiving structure or on the interface. Responses obtained on the source will be different and therefore of no use.* This limitation was already mentioned in [77,78] and can be understood by examining the system of Eq. (2): responses at the passive side B are caused only by forces through or onto the interface, whereas the responses at the source side A are a result of both the direct contribution of $\mathbf{f}_1$ and its reflection through the coupled subsystem B. This is further substantiated in Appendix A.

In the next sections, several approaches are discussed that yield a set of equivalent forces from operational tests, following the definition of Eq. (12).

3.3.2. Component TPA: blocked force

Consider the case where the boundary of subsystem A is rigidly fixed, as depicted in Fig. 5a. The operational excitation $\mathbf{f}_1$ is entirely portrayed by the reaction forces at the "blocked" interface $\mathbf{g}_2^{bl}$, such that the interface displacements $\mathbf{u}_2^{A} = \mathbf{0}$. A direct relation is found, leading to the following equivalent force:

$$\begin{bmatrix}\mathbf{u}_1\\ \mathbf{u}_2=\mathbf{0}\end{bmatrix} = \begin{bmatrix}\mathbf{Y}_{11}^{A} & \mathbf{Y}_{12}^{A}\\ \mathbf{Y}_{21}^{A} & \mathbf{Y}_{22}^{A}\end{bmatrix}\begin{bmatrix}\mathbf{f}_1\\ \mathbf{g}_2^{A}=-\mathbf{g}_2^{bl}\end{bmatrix} \quad\Longrightarrow\quad \begin{cases}\mathbf{g}_2^{bl} = \left(\mathbf{Y}_{22}^{A}\right)^{-1}\mathbf{Y}_{21}^{A}\mathbf{f}_1\\ \mathbf{f}_2^{eq} = \mathbf{g}_2^{bl}\end{cases} \tag{13}$$

The so-called *blocked-force TPA* is perhaps the most commonly known variant of component-based TPA methods because of its straight-forward applicability. It can be seen as an application of the Thévenin equivalent source problem [16], that found its way into popular mechanics halfway the 20th century [2,27,70]. Mathematically one can regard the blocked-force method as imposing a Dirichlet boundary condition on the active subsystem's interface.

The blocked-force method assumes the boundary to be infinitely stiff in all directions, which is in practice rarely the case.[10] Hence the accuracy of the blocked forces is highly subject to the stiffness of the boundary relative to the component at hand [77,101,102]. An additional difficulty is the measurement of rotational moments, as most commonly used sensors are unable to measure collocated 6-DoF interface loads. As a consequence, the blocked-force method is expected to perform best at the low frequency end for which the rigid boundary assumption is most valid and rotational effects are in practice least prominent.

3.3.3. Component TPA: free velocity

The direct counterpart of the blocked-force method is the *free-velocity TPA* as depicted in Fig. 5b. In this case the component's interfaces are left free, such that all vibrations are seen as "free displacements" $\mathbf{u}_2^{free}$ at the interface DoFs. From here on, equivalent forces[11] can be calculated by inverting the admittance measured at the free subsystem's interfaces, which can be understood by comparing the free displacements with the blocked force definition of Eq. (12)

$$\begin{bmatrix}\mathbf{u}_1\\ \mathbf{u}_2^{A}=\mathbf{u}_2^{free}\end{bmatrix} = \begin{bmatrix}\mathbf{Y}_{11}^{A} & \mathbf{Y}_{12}^{A}\\ \mathbf{Y}_{21}^{A} & \mathbf{Y}_{22}^{A}\end{bmatrix}\begin{bmatrix}\mathbf{f}_1\\ \mathbf{g}_2^{A}=\mathbf{0}\end{bmatrix} \quad\Longrightarrow\quad \begin{cases}\mathbf{u}_2^{free} = \mathbf{Y}_{21}^{A}\mathbf{f}_1\\ \mathbf{f}_2^{eq} = \left(\mathbf{Y}_{22}^{A}\right)^{-1}\mathbf{u}_2^{free}\end{cases} \tag{14}$$

Analogue to the blocked-force TPA, this method can be seen as a strict application of a Neumann boundary condition and is furthermore related to Norton's equivalent source theorem for electric networks [17]. Again, imposing free boundary

[10] For numerical analysis the blocked-force concept can be particularly effective to reduce a distributed load on the active component to fewer DoFs of the interfaces. This was recently demonstrated for transient simulation of offshore structures [100].

[11] If the admittances of the subsystems are available separately, one may also apply the free velocities directly, as shown in [82,103].

conditions can be troublesome as the vibrating system often needs to be mounted at one or more connection points to be able to run in operation. Therefore the method is in practice expected to perform best for frequencies well above the rigid body modes of the structure. Also note that effects such as friction and damping, which would occur at the interfaces of the assembled system, are absent in the operational measurement on the free component.

The fact that the method makes reference to free velocities rather than free displacements has an historical motive, as the former quantity is commonly applied in acoustical engineering in combination with acoustic pressure. For such acoustic problems, dynamic coupling of admittance is normally discarded. This is a fair assumption, considering that the impedance of the radiating source is much larger than the impedance of the receiving surrounding fluid, i.e. air. In structure-borne vibrations the source and the receiving system often exhibit similar dynamics, hence explicit coupling is needed. This was realised for a single-DoF problem by means of a non-dimensional coupling function in [58]. Extensions to multi-DoF systems and further discussion of this topic are found in [59–61]. As a final note, the free-velocity concept has been standardised into an ISO norm for characterisation of structure borne sound sources [80].

3.3.4. Component TPA: hybrid interface

As both above-mentioned methods pose their limitations in practice, one often prefers to conduct operational tests on an appropriate support structure. Such a coupled structure unavoidably displays its own dynamics on the interfaces, which need to be accounted for in order to render the equivalent forces independent of any connected part. Let us therefore imagine the active component fixed onto a test bench or test rig R as illustrated in Fig. 5c. Denoting the interface admittance of the test rig by $\mathbf{Y}^{\mathrm{R}}_{22}$, we obtain for the extended system of equations

$$\begin{bmatrix} \mathbf{u}^{\mathrm{A}}_1 \\ \mathbf{u}^{\mathrm{A}}_2 \\ \mathbf{u}^{\mathrm{R}}_2 \end{bmatrix} = \begin{bmatrix} \mathbf{Y}^{\mathrm{A}}_{11} & \mathbf{Y}^{\mathrm{A}}_{12} & \mathbf{0} \\ \mathbf{Y}^{\mathrm{A}}_{21} & \mathbf{Y}^{\mathrm{A}}_{22} & \mathbf{0} \\ \mathbf{0} & \mathbf{0} & \mathbf{Y}^{\mathrm{R}}_{22} \end{bmatrix} \begin{bmatrix} \mathbf{f}_1 \\ \mathbf{g}^{\mathrm{A}}_2 \\ \mathbf{g}^{\mathrm{R}}_2 \end{bmatrix} \quad \text{with} \begin{cases} \mathbf{u}^{\mathrm{A}}_2 = \mathbf{u}^{\mathrm{R}}_2 & \text{(displacement compatibility)} \\ \mathbf{g}^{\mathrm{A}}_2 = -\mathbf{g}^{\mathrm{R}}_2 & \text{(force equilibrium)} \end{cases} \tag{15}$$

After enforcing the compatibility and equilibrium conditions on the interface DoFs, a derivation similar to Section 3.1.2 can be followed to find the operational interface forces $\mathbf{g}^{\mathrm{R}}_2$. These forces are now dependent on the properties of both the active component A and the test rig R. Substituting the forces back into the second row of Eq. (15), the corresponding interface displacements $\mathbf{u}_2$ are obtained as well (the superscript is dropped because of compatibility)

$$\mathbf{g}^{\mathrm{R}}_2 = \left(\mathbf{Y}^{\mathrm{A}}_{22} + \mathbf{Y}^{\mathrm{R}}_{22}\right)^{-1} \mathbf{Y}^{\mathrm{A}}_{21} \mathbf{f}_1 \tag{16a}$$

$$\mathbf{u}_2 = \left[\mathbf{I} - \mathbf{Y}^{\mathrm{A}}_{22}\left(\mathbf{Y}^{\mathrm{A}}_{22} + \mathbf{Y}^{\mathrm{R}}_{22}\right)^{-1}\right] \mathbf{Y}^{\mathrm{A}}_{21} \mathbf{f}_1 \tag{16b}$$

Eqs. (16a) and (16b) hold for any $\mathbf{Y}^{\mathrm{R}}_{22}$, as long as no external force is acting on the test rig. The desired set of equivalent forces equation (12) is obtained by combining Eqs. (16a) and (16b) in such way that the dynamics of the test rig $\mathbf{Y}^{\mathrm{R}}_{22}$ are eliminated

$$\mathbf{f}^{\mathrm{eq}}_2 = \left(\mathbf{Y}^{\mathrm{A}}_{22}\right)^{-1} \mathbf{Y}^{\mathrm{A}}_{21} \mathbf{f}_1 \quad \Longrightarrow \quad \mathbf{f}^{\mathrm{eq}}_2 = \mathbf{g}^{\mathrm{R}}_2 + \left(\mathbf{Y}^{\mathrm{A}}_{22}\right)^{-1} \mathbf{u}_2 \tag{17}$$

As it turns out, Eq. (17) forms the sum of contributions of both the blocked force and the free velocity experiment, respectively, Eqs. (13) and (14). One could therefore speak of a *hybrid interface* condition, or Robin boundary condition in a mathematical sense. It can indeed be verified that Eqs. (16a) and (16b) converge[12] to the blocked forces for $\mathbf{Y}^{\mathrm{R}} \to \mathbf{0}$ and to free velocities when $\mathbf{Y}^{\mathrm{R}} \to \infty$.

The hybrid interface approach combining force and motion was originally published in [78]; the displacement term was regarded in this work as the “non-rigid test bench compensation” to the imperfect blocked forces. Although generally applicable in theory, it should be mentioned that the method can be rather costly and time-consuming in practice, as one needs to explicitly measure collocated forces and motion in all directions for every interface node [101].

In lack of force measurement, one may substitute the third row of (15) for $\mathbf{g}^{\mathrm{B}}_2$. The so obtained approach was suggested in [102] and takes displacement measurement only

$$\mathbf{f}^{\mathrm{eq}}_2 = \left(\mathbf{Y}^{\mathrm{R}}_{22}\right)^{-1} \mathbf{u}_2 + \left(\mathbf{Y}^{\mathrm{A}}_{22}\right)^{-1} \mathbf{u}_2 \tag{18}$$

The price for not having to measure interface forces is that separate FRF measurements should now be conducted, to obtain the subsystem admittances of the active component and the test rig.

3.3.5. Component TPA: in situ

Looking again at Eq. (18) we observe that the two inverted admittance FRF matrices in fact represent the dynamic stiffness matrices of respectively component A and R for the same set of collocated interface DoFs. They can be combined by

[12] A intuitive presentation of the range between the two limit cases is given in [61].

simple impedance addition[13]

$$\mathbf{f}_2^{\mathrm{eq}} = \left(\mathbf{Z}_{22}^{\mathrm{R}} + \mathbf{Z}_{22}^{\mathrm{A}}\right)\mathbf{u}_2 = \mathbf{Z}_{22}^{\mathrm{AR}}\mathbf{u}_2 \tag{19}$$

The result of Eq. (19) is indeed indifferent to the dynamics of R or any other mounting structure that component A is connected to. Transforming back to admittance notation, we find that the blocked forces can be calculated inversely from the admittance of the assembly's interface or, in an overdetermined fashion, using a sufficient set of indicator points $\mathbf{u}_4$ on the receiving subsystem

$$\mathbf{f}_2^{\mathrm{eq}} = \left(\mathbf{Y}_{22}^{\mathrm{AR}}\right)^{-1}\mathbf{u}_2 \quad \text{or} \quad \mathbf{f}_2^{\mathrm{eq}} = \left(\mathbf{Y}_{42}^{\mathrm{AR}}\right)^{+}\mathbf{u}_4 \tag{20}$$

Obtained from a different derivation, the approach of Eq. (20) has first been proposed by Moorhouse and Elliott [62,63] as the *in situ* method. As implied by the name, the operational measurement may even be conducted in the target assembly AB, avoiding dismounting of any part, namely

$$\mathbf{f}_2^{\mathrm{eq}} = \left(\mathbf{Y}_{22}^{\mathrm{AB}}\right)^{-1}\mathbf{u}_2 \quad \text{or} \quad \mathbf{f}_2^{\mathrm{eq}} = \left(\mathbf{Y}_{42}^{\mathrm{AB}}\right)^{+}\mathbf{u}_4 \tag{21}$$

The equivalent forces resulting from application of Eq. (21) are nonetheless a property of component A only and thus transferable to an assembly with another passive side.

The in situ force determination procedure is illustrated in Fig. 5d. Indeed, Eq. (21) represents the inverse of Eq. (11) yet with an extended set of response DoFs in order to render the system (over) determined and thus invertible. As a consequence, the method shows great resemblance with the classical matrix-inverse method of Eq. (10) the difference being the choice for the assembled admittance instead of the passive subsystem's admittance. Similar techniques regarding matrix conditioning (e.g. over-determination, singular value rejection) apply as well to the in situ method. Most remarkable is that the receiving side can be chosen arbitrarily, as the equivalent forces identified by Eq. (20) or (21) are theoretically invariant of any subsystem coupled to it. In that respect, two important conditions need to be kept in mind:

1. Operational excitations $\mathbf{f}_1$ may only originate from the domain of component A. Any excitation coming from the passive side will disturb the determination of equivalent forces.
2. Although the responses used for the matrix inversion ($\mathbf{u}_2$ or $\mathbf{u}_4$) can be positioned rather arbitrarily, they are bounded to the domain of the interface and the passive side. This relates back to the remark made after Eq. (12) and discussed in Appendix A: vibrations at the source structure are not only caused by the interface forces but also by the source excitations directly.

Physically one could interpret the in situ method as follows: knowing the transfer functions from the interface DoFs to several points on the passive side, Eq. (20) or (21) seeks for a set of equivalent forces $\mathbf{f}_2^{\mathrm{eq}}$ that, applied to the interface DoFs of the assembled structure, generates the same responses $\mathbf{u}_4$ at the passive side. Given that this response set is overdetermined, the equivalent forces are calculated such that they minimise the sum of the squared errors (or l^2-norm) in the extended set[14] $\mathbf{u}_4$.

Several numerical and experimental studies of in situ source characterisation have been reported [98,102,107–110]. A time-domain force reconstruction algorithm was proposed by Sturm [111,112]; see also Section 4.5. Further generalisation of the in situ concept can be recognised in the *pseudo-forces* method that is discussed next.

3.3.6. Component TPA: pseudo-forces

The last member of the component-based TPA family to discuss is the *pseudo-forces* method as proposed by Janssens and Verweij in the late 1990s [64,65,113]. It assumes the existence of a non-unique set of pseudo-forces acting on the outer surface of the active component, cancelling out the effect of the operational vibrations transmitted through the interface to the passive side. This is illustrated in Fig. 6a. If those forces are now applied in the opposite direction to the assembly with the source shut-down, an identical response at the receiving side should be obtained, see Fig. 6c. In other words, the pseudo-forces are supposed to represent the source excitation for responses at the passive side.

The fact that it can be regarded as a component TPA method lies in the former assumption: if there exists a set of pseudo-forces that cancels out the operational dynamics at the interface, the responses beyond this interface shall be zero as well, hence these forces are invariant of any structure attached to it. A similar reasoning may as well be applied to the previously discussed equivalent force methods, yet the locations of the pseudo-forces are not bounded to the interface but extend to the full domain of the active component (see Fig. 6).

The actual determination of the pseudo-forces is carried out slightly differently. The first step is to define a set of s pseudo-forces $\mathbf{f}_{\mathrm{ps}}$ on the active component that is (a) sufficient to represent the excitation source and (b) easily accessible for impact hammer or shaker measurement. One could think of a minimum of $s=6$ forces when the interface behaviour can be considered as rigid, or a larger number in case of more intricate connectivity. Secondly, a set of $n \geq s$ indicator response DoFs has to be chosen on the passive side from which the operational excitation is monitored. These responses are denoted

[13] This is standard practice for FEM assembly.

[14] Similar ideas are used in the field of experimental substructure decoupling: the identification of the force that decouples the residual substructure can be improved by defining an “extended interface”, adding some additional DoFs on the structure of interest distant from the interface [104–106].

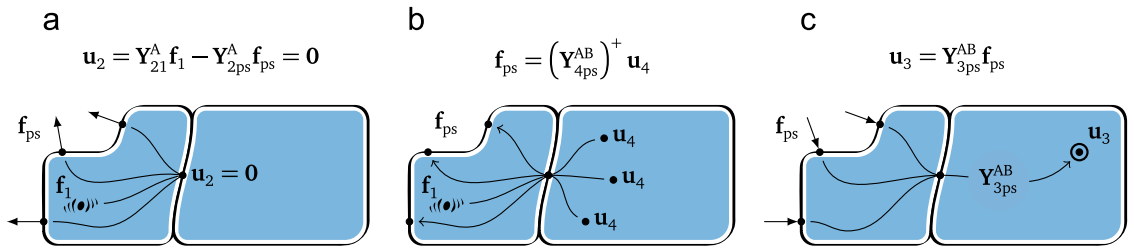

Fig. 6. The concept of the pseudo-forces component TPA method. (a) Pseudo-forces cancelling out the operational excitation at the interface. (b) Inverse determination of the pseudo-forces under operation. (c) Application of pseudo-forces to the assembly, causing the same response.

by $\mathbf{u}_4$ and can be written as a result of $\mathbf{f}_1$, similar to Eq. (9)

$$\mathbf{u}_4 = \mathbf{Y}^{\mathrm{AB}}_{41}\mathbf{f}_1 = \mathbf{Y}^{\mathrm{B}}_{42}\left(\mathbf{Y}^{\mathrm{A}}_{22}+\mathbf{Y}^{\mathrm{B}}_{22}\right)^{-1}\mathbf{u}^{\mathrm{free}}_{2,\mathbf{f}_1} \quad \text{with } \mathbf{u}^{\mathrm{free}}_{2,\mathbf{f}_1} \triangleq \mathbf{Y}^{\mathrm{A}}_{21}\mathbf{f}_1 \tag{22a}$$

A substitution is made here using the free velocity caused by the excitation $\mathbf{f}_1$, or in other words: the theoretical motion at the interface of component A if the interfaces were left free, see also Section 3.3.3. This is by no means a quantity that needs to be measured, but will prove useful for the derivation later on.

The next step is to determine pseudo-forces $\mathbf{f}_{ps}$ that best recreate the operational responses at the indicator DoFs $\mathbf{u}_4$ when the source excitation is shut down. Note that the assumption is similar to the equivalent forces problem stated in Section 3.3.1, yet the pseudo-forces act on the outer surface of the active component rather than its interfaces. Similar to Eq. (22a), the response at the indicator DoFs as a result of the pseudo-forces reads

$$\mathbf{u}_4 = \mathbf{Y}^{\mathrm{AB}}_{4ps}\mathbf{f}_{ps} = \mathbf{Y}^{\mathrm{B}}_{42}\left(\mathbf{Y}^{\mathrm{A}}_{22}+\mathbf{Y}^{\mathrm{B}}_{22}\right)^{-1}\mathbf{u}^{\mathrm{free}}_{2,\mathbf{f}_{ps}} \quad \text{with } \mathbf{u}^{\mathrm{free}}_{2,\mathbf{f}_{ps}} \triangleq \mathbf{Y}^{\mathrm{A}}_{21}\mathbf{f}_{ps} \tag{22b}$$

Now, the pseudo-forces $\mathbf{f}_{ps}$ that best describe the operational source excitations are found from solving an overdetermined system with the response set $\mathbf{u}_4$ that was measured under operation (see Fig. 6b)

$$\mathbf{f}_{ps} = \left(\mathbf{Y}^{\mathrm{AB}}_{4ps}\right)^{+}\mathbf{u}_4 \tag{23}$$

It can be shown that these forces, under certain conditions, are a property of component A only. A sufficient condition is that the free interface velocities $\mathbf{u}^{\mathrm{free}}_2$ as a result of the original source excitation can be fully represented by the set of pseudo-forces determined from Eq. (23). In that case the definitions of Eqs. (22a) and (22b) may be equated and one finds that the pseudo-forces are specific for the source component

$$\mathbf{u}^{\mathrm{free}}_{2,\mathbf{f}_{ps}} = \mathbf{u}^{\mathrm{free}}_{2,\mathbf{f}_1} \quad \Longrightarrow \quad \mathbf{f}_{ps} = \left(\mathbf{Y}^{\mathrm{A}}_{2ps}\right)^{+}\mathbf{Y}^{\mathrm{A}}_{21}\mathbf{f}_1 \tag{24}$$

Applying these pseudo-forces to the FRFs of an assembled system of interest, i.e. $\mathbf{Y}^{\mathrm{AB}}_{3ps}$, it can be verified that the correct receiver responses $\mathbf{u}_3$ at the passive side are obtained

$$\mathbf{u}_3 = \mathbf{Y}^{\mathrm{AB}}_{3ps}\mathbf{f}_{ps} = \left[\mathbf{Y}^{\mathrm{B}}_{32}\left(\mathbf{Y}^{\mathrm{A}}_{22}+\mathbf{Y}^{\mathrm{B}}_{22}\right)^{-1}\mathbf{Y}^{\mathrm{A}}_{2ps}\right]\left(\mathbf{Y}^{\mathrm{A}}_{2ps}\right)^{+}\mathbf{Y}^{\mathrm{A}}_{21}\mathbf{f}_1 = \mathbf{Y}^{\mathrm{AB}}_{31}\mathbf{f}_1 \tag{25}$$

The pseudo-forces determined from Eq. (23) are indeed transferable to an assembly with another passive side. Eq. (25) yields the responses for this new assembly, provided that the columns of the FRF matrix $\mathbf{Y}^{\mathrm{AB}}_{3ps}$ correspond to the same pseudo-forces, i.e. excitation points at the source.

The previously discussed in situ method can be regarded as a special case of the pseudo-force method, namely for the case where the pseudo-forces are located at the interfaces. The pseudo-forces calculated from Eq. (23) shall then equal the equivalent (blocked) forces from Eq. (12), namely $\mathbf{f}_{ps} = \mathbf{f}^{\mathrm{eq}}_2$. With regard to the positioning of the indicator DoFs $\mathbf{u}_4$, the same restriction holds as for the in situ method, namely that they must be located at the passive system B or at the interface.[15]

A related idea was proposed [78] to calculate pseudo-forces (or *substitute forces* in the original work) from equivalent forces that were in turn obtained from test bench measurements

$$\mathbf{f}_{ps} = \left(\mathbf{Y}^{\mathrm{A}}_{2ps}\right)^{+}\mathbf{Y}^{\mathrm{A}}_{22}\mathbf{f}^{\mathrm{eq}}_2$$

To find the receiver responses $\mathbf{u}_3$, Eq. (25) can now be applied instead of Eq. (11). This is useful if $\mathbf{Y}^{\mathrm{AB}}_{32}$ is unmeasurable, namely when the interfaces of the assembled system AB are inaccessible for FRF measurement.

[15] This was erroneously stated in the original work [65].

3.4. Transmissibility-based TPA

The two previously discussed families of TPA have in common that they attempt to model the vibration transmission in a physically correct sense, namely by determining as many forces and moments as required to describe the subsystem connectivity in full. Consequently, both families explicitly require the corresponding FRFs for the interface DoFs to the receiving response locations. It is evident that this approach ultimately reveals a wealth of information on the particular functioning of the active component, force distribution over the interface, resonances in the structure, etc. If however the mere purpose of a TPA is to identify the dominant path contributions in the assembled product, the efforts to set up and conduct the full experiment can be fairly disproportionate and costly. This is especially the case when multiple incoherent vibration sources are to be investigated.

The last family to discuss avoids the stage of explicit force determination. Instead the path contributions are determined from so-called "transmissibilities" between sensors, possibly calculated from operational measurements. Various methods are discussed in the following sections that share the following properties:

1. Measurements are conducted on the assembled product only, saving time to dismount the active components. In fact the interfaces between the active and passive components are no longer of principal interest.
2. Path contributions are determined from well-chosen indicator points around the sources or connections. These indicator points function as inputs to the TPA.
3. The result of the analysis is highly subject to the choice for these indicator points; care should therefore be taken to include all transmission paths.

The family of *transmissibility-based TPA* methods indeed departs from the traditional source-transfer-receiver model that assumes a physically meaningful set of loads, FRFs and responses. Although potentially less accurate, methodologies derived from this concept tend to be easy to set up, versatile concerning sensor type and particularly effective for ranking contributions from several sources. From a practical point of view, transmissibility-based TPA tries to outrun the physically correct methods by its ability to conduct multiple cycles in shorter time. Nevertheless, under certain conditions, results of similar (or even equivalent) accuracy can be achieved with classical and component-based TPA methods.

3.4.1. The transmissibility concept

To discuss the theoretical concepts behind transmissibility-based methods, consider an assembled system AB with two connection points[16] as shown in Fig. 7. The active side contains a vibration mechanism that is characterised by internal forces $\mathbf{f}_1$; the receiver responses at the passive side are denoted by p DoFs in $\mathbf{u}_3$. To monitor the vibrations transmitted across the interfaces, n indicator DoFs $\mathbf{u}_4$ are positioned around the connection points.

Let us first assume that the source excitation $\mathbf{f}_1$ can be described by o forces (or independent force distributions) and that FRFs are measurable for all of the above-mentioned DoFs. The equations for the passive-side responses then read

$$\begin{cases} \mathbf{u}_3 = \mathbf{Y}_{31}^{AB}\mathbf{f}_1 & \text{for } p \text{ receiver DoFs} \quad (26a) \\ \mathbf{u}_4 = \mathbf{Y}_{41}^{AB}\mathbf{f}_1 & \text{for } n \text{ indicator DoFs} \quad (26b) \end{cases}$$

Provided that $n \geq o$ and $\mathbf{Y}_{41}^{AB}$ is full rank, all excitation forces $\mathbf{f}_1$ are observable from $\mathbf{u}_4$. Hence Eq. (26b) can be inverted and substituted into Eq. (26a). The responses $\mathbf{u}_3$ are now expressed in terms of the DoFs $\mathbf{u}_4$ that can be measured under operation:

$$\mathbf{u}_3 = \mathbf{T}_{34,\mathbf{f}_1}^{AB}\mathbf{u}_4 \quad \text{with } \mathbf{T}_{34,\mathbf{f}_1}^{AB} \triangleq \mathbf{Y}_{31}^{AB}\left(\mathbf{Y}_{41}^{AB}\right)^{+} \tag{27}$$

The so obtained transmissibility matrix $\mathbf{T}_{34,\mathbf{f}_1}^{AB}$ relates motion at the indicator DoFs $\mathbf{u}_4$ (the inputs) to the receiver DoFs $\mathbf{u}_3$ (the outputs) for excitation forces $\mathbf{f}_1$. Interestingly, the size of the transmissibility matrix has become $p \times n$, obfuscating the o excitations associated with the original FRFs. This raises the question which excitations are really needed to construct the transmissibility matrix and to what extend this matrix is generally valid for the problem ($\mathbf{u}_4 \rightarrow \mathbf{u}_3$) under different excitations of the source structure.

To gain more insight in the transmissibility problem stated by Eq. (27), let us expand Eqs. (26a) and (26b) in terms of the subsystems' admittances. As seen in previous derivations, the terms that couple the subsystems are identical for all responses ($\mathbf{u}_3, \mathbf{u}_4$) at the passive side

$$\begin{bmatrix} \mathbf{u}_3 \\ \mathbf{u}_4 \end{bmatrix} = \begin{bmatrix} \mathbf{Y}_{31}^{AB} \\ \mathbf{Y}_{41}^{AB} \end{bmatrix}\mathbf{f}_1 = \begin{bmatrix} \mathbf{Y}_{32}^{B} \\ \mathbf{Y}_{42}^{B} \end{bmatrix}\left(\mathbf{Y}_{22}^{A} + \mathbf{Y}_{22}^{B}\right)^{-1}\mathbf{Y}_{21}^{A}\mathbf{f}_1$$

[16] An example with two connection points was chosen here merely to provide better insight into some important cross-correlation properties. There is no fundamental consequence for the generality of the methods derived.

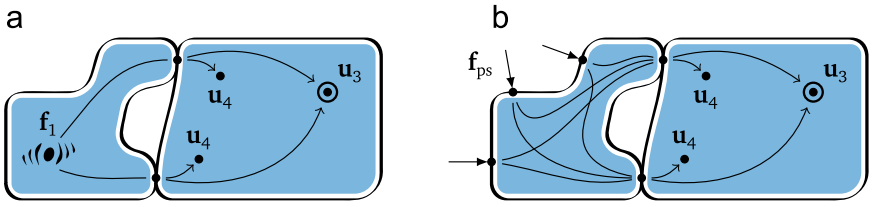

Fig. 7. The transmissibility concept for an example with two connection points. (a) Transmissibility from source FRFs. (b) Transmissibility from alternative FRFs.

Recalling now the expressions for the interface force and free velocity, respectively Eqs. (4) and (14), the following substitutions can be made:

$$\begin{bmatrix}\mathbf{u}_3\\ \mathbf{u}_4\end{bmatrix} = \begin{bmatrix}\mathbf{Y}^{\mathrm{B}}_{32}\\ \mathbf{Y}^{\mathrm{B}}_{42}\end{bmatrix}\mathbf{g}^{\mathrm{B}}_2 \quad \text{with} \begin{cases}\mathbf{g}^{\mathrm{B}}_2 = \left(\mathbf{Y}^{\mathrm{A}}_{22}+\mathbf{Y}^{\mathrm{B}}_{22}\right)^{-1}\mathbf{u}^{\mathrm{free}}_2 & \text{for } m \text{ interface forces}\\ \mathbf{u}^{\mathrm{free}}_2 = \mathbf{Y}^{\mathrm{A}}_{21}\mathbf{f}_1 & \text{for } m \text{ free velocities}\end{cases} \tag{28}$$

Hence, Eq. (28) shows that the transmission of vibrations from o forces $\mathbf{f}_1$ to n responses $\mathbf{u}_4$ is limited by the number of DoFs of the interface forces/displacements m. This means that the interface acts as a *bottleneck*: it limits the effective rank of the transmissibility problem to a maximum of m. Furthermore, Eq. (28) exposes two interesting properties of the transmissibility concept:

1. Regarding the source excitation, Eq. (28) shows a direct relation between the interface forces $\mathbf{g}^{\mathrm{B}}_2$ of the coupled system and the theoretical free velocities $\mathbf{u}^{\mathrm{free}}_2$ at the disconnected interfaces of component A. As understood from the component-based TPA methods, various sets of forces can be defined that equivalently produce these free interface velocities $\mathbf{u}^{\mathrm{free}}_2$, such as the pseudo-forces of Eq. (22b). This is illustrated in Fig. 7b. In fact, any set of forces on the source that renders the interface fully *controllable* will guarantee convergence to a transmissibility matrix that generally captures the transmission of vibrations caused in component A. This property is used in the operational TPA method as discussed in the next section.
2. Regarding the transmissibility, the problem ($\mathbf{u}_4 \rightarrow \mathbf{u}_3$) is in fact *specific to the passive side only*, provided that the interface forces $\mathbf{g}^{\mathrm{B}}_2$ are fully observable from $\mathbf{u}_4$. That means that the second line of Eq. (28) can be inverted, which is equivalent to Eq. (10) from the classical matrix-inverse method. With respect to transmissibility-based TPA, it implies that if $\mathbf{u}_4$ is chosen in such way that all interface forces are *observable*, $\mathbf{g}^{\mathrm{B}}_2$ can be eliminated from Eq. (28) and the transmissibility matrix becomes a property of the passive side only, namely

$$\mathbf{u}_3 = \mathbf{T}^{\mathrm{B}}_{34}\mathbf{u}_4 \quad \text{with } \mathbf{T}^{\mathrm{B}}_{34} \triangleq \mathbf{Y}^{\mathrm{B}}_{32}\left(\mathbf{Y}^{\mathrm{B}}_{42}\right)^{+} \tag{29}$$

   An elegant duality can be observed here with the component-based TPA concept that characterises the excitation as a property of the source component. More properties of the transmissibility matrix are discussed in [45,114].

Theoretically, it can be stated that the controllability is a property of the source component A, whereas the observability is specific to the receiving structure B. If both conditions are satisfied, Eqs. (27) and (29) generate the same transmissibility matrix, hence $\mathbf{T}^{\mathrm{AB}}_{34} = \mathbf{T}^{\mathrm{B}}_{34}$ or simply $\mathbf{T}_{34}$. The pseudo-inversion step involved in Eqs. (27) and (29) "decorrelates" the transmissibility columns associated with $\mathbf{u}_4$ into linearly independent contributions to the receiver DoFs $\mathbf{u}_3$, such that an element of $\mathbf{T}_{34}$ is defined as follows:

$$T_{ij} \triangleq \left.\frac{u_i}{u_j}\right|_{u_{k\neq j}=0} \quad \begin{cases} u_i \in \mathbf{u}_3 \\ u_j, u_k \in \mathbf{u}_4 \end{cases}$$

This process is often referred to as Cross-Talk Cancellation (CTC). Note that this concerns a spatial or "modal" decorrelation[17] only, just like other methods involving FRF matrix inversion. It should therefore by no means be understood as some special signal processing step.

In practice, to obtain $\mathbf{T}_{34}$ from FRFs as illustrated by Fig. 7a or b, one requires sufficient excitations and indicator DoFs to respectively *control* and *observe* the dynamics at the interface. However the foremost reason for using a transmissibility-based TPA method is to identify source path contributions without the need to conduct a tedious FRF measurement campaign. The next section discusses how to obtain $\mathbf{T}_{34}$ from operational responses only.

3.4.2. *Operational transfer path analysis (OTPA)*

The transmissibility matrix $\mathbf{T}_{34}$ can be estimated statistically from the correlation between $\mathbf{u}_3$ and $\mathbf{u}_4$ when monitored under a variety of operational test conditions. The fundamental assumption is that, by testing the vibration source under different operational conditions (e.g a motor operating at different speeds or torques), multiple load cases are exercised that are slightly independent.

[17] This decorrelation has been approached in several ways: for instance based on so-called global and direct transmissibility functions (GTDT) in the work of Magrans and Guasch [42–45] or along conventional FRFs as seen in Varoto and McConnell and Ribeiro et al. [48–51].

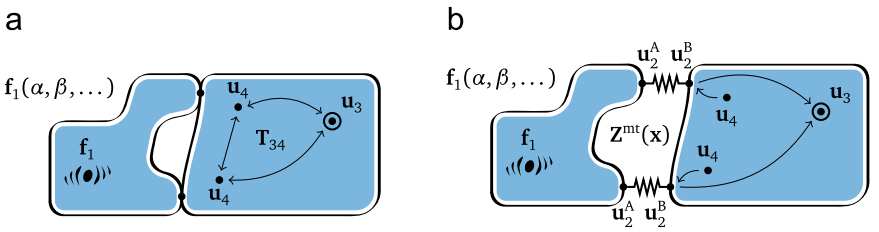

Fig. 8. Transmissibility-based TPA approaches; the source excitation $\mathbf{f}_1$ depends on operational parameters $(\alpha,\beta,\dots)$ such as engine speed or torque. (a) Operational TPA. (b) OPAX.

However, as seen in the previous section, the effect of these load cases across the interface is theoretically limited to a maximum of m independent modes of vibration at the passive side, because of the bottleneck-effect of the interface. This is further discussed below.

Let us now assume that the operational excitation is able to generate sufficient independent load cases $\mathbf{f}_1(\alpha,\beta\dots)$, where α and β represent independent operational parameters.[18] This is illustrated in Fig. 8a. Eq. (27) can be established for r sets of measured responses obtained under different operational conditions, e.g. the sliced time-blocks of a run-up measurement. This amounts to stacking the r measured spectra of the receiving DoFs and indicator DoFs column-wise into arrays $\mathbf{U}_3$ and $\mathbf{U}_4$ to construct the following system of equations (the superscript on $\mathbf{u}$ indicates the measurement block number)

$$\underbrace{\left[\mathbf{u}_3^{(1)}\ \mathbf{u}_3^{(2)}\ \cdots\ \mathbf{u}_3^{(r)}\right]}_{p\times r} = \underbrace{\mathbf{T}_{34}}_{p\times n}\underbrace{\left[\mathbf{u}_4^{(1)}\ \mathbf{u}_4^{(2)}\ \cdots\ \mathbf{u}_4^{(r)}\right]}_{n\times r} \quad\Longrightarrow\quad \mathbf{U}_3=\mathbf{T}_{34}\mathbf{U}_4 \tag{30}$$

When sufficient measurement data is acquired to ensure $r\geq n$, the problem of Eq. (30) can be made invertible by post-multiplying with $\mathbf{U}_4^H$. The transmissibility matrix is then found from solving this system or, more conveniently, from the H_1 estimator[19] of the cross-power spectra (CPS) and auto-power spectra (APS) of the measured DoFs

$$\mathbf{T}_{34}=\mathbf{U}_3\mathbf{U}_4^H\left(\mathbf{U}_4\mathbf{U}_4^H\right)^{-1} \quad\Longrightarrow\quad \mathbf{T}_{34}=\mathbf{S}_{34}\mathbf{S}_{44} \quad \text{with} \begin{cases} \mathbf{S}_{34}=\frac{1}{r}\mathbf{U}_3\mathbf{U}_4^H & \text{(CPS)} \\ \mathbf{S}_{44}=\frac{1}{r}\mathbf{U}_4\mathbf{U}_4^H & \text{(APS)} \end{cases} \tag{31}$$

Eq. (31) performs cross-talk cancellation similar to Eq. (27). Now that the transmissibility matrix $\mathbf{T}_{34}$ has been estimated globally, the actual path contributions can be analysed for each measurement cycle. If performed correctly (i.e. all transfer paths were included), the reconstructed response spectra equal the response spectra that were measured directly

$$\mathbf{u}_3^{(l)}=\mathbf{T}_{34}\mathbf{u}_4^{(l)}, \quad l\in\{1,\dots,r\} \tag{32}$$

The approach governed by Eqs. (30) and (31) is generally known as *Operational Transfer Path Analysis* (OTPA) [53]. Clearly, the performance of this method is subject to the choice and positioning of the indicator sensors $\mathbf{u}_4$, that function as "inputs" to the analysis. Too few sensors (or too distant from the source connections) could lead to neglecting important transmission paths, resulting in unrealistic prognoses [117]. On the other hand, having too many sensors (or too close to each other) might complicate the inversion of $\mathbf{S}_{44}$ due to poor conditioning, resulting in amplification of measurement noise [118].

Theoretically, the rank of $\mathbf{U}_4$ is limited by the number of DoFs at the interface m. This implies that $\mathbf{U}_4$ and thus $\mathbf{S}_{44}$ is rank deficient, even if $r>n$. It is therefore common practice to perform a Principal Component Analysis (PCA) in order to identify how many independent modes of vibration are present in the system and transferred across the interfaces. Principle components are calculated from the singular value decomposition of $\mathbf{U}_4$. The left-singular vectors represent the vibration mode shapes that build up to the vibrations in the indicator DoFs, sorted from the largest contribution to the smallest. By controlling the amount of principle components that are used in the computation of the transmissibility by Eq. (31), the condition number can be kept low such that one balances between the completeness of path descriptions and attenuation of measurement noise. This is not discussed in detail here, guidelines can be found in specific literature on OTPA [53,55,119].

Another strong advantage of OTPA is the ease of combining various types of sensors, both for the input (indicator) and output (receiver) DoFs. Quantities such as accelerations, velocities, sound pressures and even forces and strains can be used in a mixed fashion, as long as proper scaling (unit normalisation) is taken into account [53]. This makes OTPA a suitable method to quickly investigate the proportion of structure-borne and airborne contributions [120]. Other related extensions or applications include Response Modification Analysis (RMA) for providing structural sensitivities to the target responses [57], pass-by analysis of road vehicle noise [121,122] and time-domain auralisation of OTPA, sometimes referred to as Transfer Path Synthesis (TPS) [123].

[18] In [115] it is suggested that external excitation on the source structure, e.g. by use of a non-instrumented hammer, leads to better conditioning of the transmissibility matrix compared to a sequence of operational excitations. This resembles the approach depicted in Fig. 7b.

[19] The H_1 estimator is a well-known principle in experimental modal analysis to determine FRFs from a multiple input–output (MIMO) test, see for instance [32,35]. Alternative ways to obtain the transmissibility matrix have recently been explored, such as the H_2 or H_s estimator to balance the error contributions between the inputs and outputs [116].

3.4.3. Operational mount identification (OPAX)

The Operational Path Analysis with eXogenous Inputs (OPAX) [124,125] is a hybrid TPA method that aims at combining the physical understanding gained from classical TPA methodology with the identification potential of operational TPA principles. OPAX combines the classical mount-stiffness and matrix-inverse TPA principles as discussed in Sections 3.2.2 and 3.2.3, but adds the ability to estimate mount stiffness parameters from operational tests. Regarding these mount parameters, a mount model can be selected that fits the system under test and yields the right balance between analysis time/accuracy that was targeted for. This way the OPAX method can be adjusted to suit systems with resilient mounts as well as rigid connections and include airborne paths in the analysis with similar ease.

In what follows, an interpretation of the original publication [125] is presented step-by-step, such that it fits in the proposed framework. A schematic overview of the subsystems instrumentation is provided in Fig. 8b.

Classical mount-stiffness scheme: Central to the OPAX method stands the classical TPA assumption, stating that passive side responses are obtained by application of operational interface forces to the FRFs of subsystem B, similar to Eq. (6). The interface forces are modelled as the product of mount-stiffnesses in $\mathbf{Z}^{\mathrm{mt}}$ and the differential interface displacements between the active and the passive side, as in Eq. (8). Let us write the corresponding equations for the receiver responses $\mathbf{u}_3$ and additional indicator DoFs $\mathbf{u}_4$

$$\begin{bmatrix}\mathbf{u}_3\\ \mathbf{u}_4\end{bmatrix} = \begin{bmatrix}\mathbf{Y}^{\mathrm{B}}_{32}\\ \mathbf{Y}^{\mathrm{B}}_{42}\end{bmatrix}\mathbf{g}^{\mathrm{B}}_2 \tag{33}$$

and for the interface forces

$$\mathbf{g}^{\mathrm{B}}_2 = \mathbf{Z}^{\mathrm{mt}}\left(\mathbf{u}^{\mathrm{A}}_2 - \mathbf{u}^{\mathrm{B}}_2\right) \tag{34a}$$

One of the aims of OPAX is to identify the mount stiffnesses $\mathbf{Z}^{\mathrm{mt}}$ from operation tests. It is assumed that the mounts do not exhibit cross-directional effects, such that $\mathbf{Z}^{\mathrm{mt}}$ is a diagonal matrix. Eq. (34a) can therefore be reformulated using the element-wise or Hadamard product of the set of m single-DoF mount stiffnesses and the differential displacements across the mounts in the corresponding directions

$$\mathbf{g}^{\mathrm{B}}_2 = \left(\mathbf{u}^{\mathrm{A}}_2 - \mathbf{u}^{\mathrm{B}}_2\right)\circ\mathbf{z}^{\mathrm{mt}} \quad \text{with } \mathbf{z}^{\mathrm{mt}} = \begin{bmatrix} z^{\mathrm{mt}}_1 & \cdots & z^{\mathrm{mt}}_m\end{bmatrix}^T \tag{34b}$$

Mount parametrisation: The next step is to define a model to parametrise the mount stiffnesses in $\mathbf{z}^{\mathrm{mt}}(\omega)$. As suggested in the original work [125], one can choose a single-DoF mount model consisting of linear mass, damping and stiffness terms (m, c, k) or a frequency-dependent model that accommodates for constant dynamic stiffness (z_b) in selected frequency bands. Both models are illustrated in Fig. 9.

Let us continue the discussion with the single-DoF mount model. This model introduces $q=3$ unknowns per interface DoF, contained in the parameter set $\mathbf{x}^{(1)}$

$$z^{\mathrm{mt}}_1(\omega) = f\left(\omega, \mathbf{x}^{(1)}\right) = \begin{bmatrix} -\omega^2 & j\omega & 1\end{bmatrix}\begin{bmatrix} m\\ c\\ k\end{bmatrix}^{(1)} = \psi(\omega)\mathbf{x}^{(1)} \tag{35a}$$

It is important to note that $\mathbf{x}^{(1)}$ is a *frequency independent* parametrisation of the stiffness $z^{\mathrm{mt}}_1(\omega)$ of mount DoF with index 1; the frequency dependent part is governed by $\psi(\omega)$ which is common for all DoFs. Extending now for all m interface forces, the system reads

$$\underbrace{\begin{bmatrix} z^{\mathrm{mt}}_1(\omega)\\ \vdots\\ z^{\mathrm{mt}}_m(\omega)\end{bmatrix}}_{m\times 1} = \underbrace{\begin{bmatrix} -\omega^2 & j\omega & 1 & & & \\ & & \ddots & & & \\ & & & -\omega^2 & j\omega & 1\end{bmatrix}}_{m\times qm}\underbrace{\begin{bmatrix}\mathbf{x}^{(1)}\\ \vdots\\ \mathbf{x}^{(m)}\end{bmatrix}}_{qm\times 1} \quad\Longrightarrow\quad \mathbf{z}^{\mathrm{mt}}(\omega) = \mathbf{\Psi}(\omega)\mathbf{x} \tag{35b}$$

Different mount models can be imagined, such as the multi-band model as mentioned before and functions of higher-order polynomials as long as $\mathbf{x}$ can be written as frequency-independent parameters. A priori available mount stiffness parameters can also be implemented in Eq. (35b).

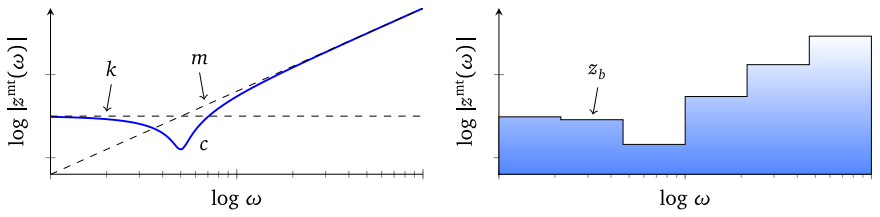

Fig. 9. Two mount models: based on m, c, k properties (left) and multi-band (right).

Identification of mount parameters: Substituting Eqs. (34b) and (35b) into the original classic TPA scheme of Eq. (33), a system of equations is obtained that includes the parametrised mount model

$$\begin{bmatrix}\mathbf{u}_3(\omega)\\ \mathbf{u}_4(\omega)\end{bmatrix} = \begin{bmatrix}\mathbf{Y}^{\mathrm{B}}_{32}(\omega)\\ \mathbf{Y}^{\mathrm{B}}_{42}(\omega)\end{bmatrix} \underbrace{\left(\mathbf{u}^{\mathrm{A}}_2(\omega)-\mathbf{u}^{\mathrm{B}}_2(\omega)\right)\circ\boldsymbol{\Psi}(\omega)\mathbf{x}}_{\approx\mathbf{g}^{\mathrm{B}}_2} \tag{36}$$

The aim is now to construct a standard linear system of equations that allows us to solve for $\mathbf{x}$. Let us first collect all frequency-dependent terms into matrices $\mathbf{A}(\omega)$. These include the FRFs of the passive subsystem and the interface displacements measured under operational tests

$$\begin{bmatrix}\mathbf{u}_3(\omega)\\ \mathbf{u}_4(\omega)\end{bmatrix} = \begin{bmatrix}\mathbf{A}_3(\omega)\\ \mathbf{A}_4(\omega)\end{bmatrix}\mathbf{x} \quad \text{with} \quad \begin{cases}\mathbf{A}_3(\omega)=\mathbf{Y}^{\mathrm{B}}_{32}\left(\mathbf{u}^{\mathrm{A}}_2-\mathbf{u}^{\mathrm{B}}_2\right)\circ\boldsymbol{\Psi}(\omega) & [p\times \mathrm{qm}]\\ \mathbf{A}_4(\omega)=\mathbf{Y}^{\mathrm{B}}_{42}\left(\mathbf{u}^{\mathrm{A}}_2-\mathbf{u}^{\mathrm{B}}_2\right)\circ\boldsymbol{\Psi}(\omega) & [n\times \mathrm{qm}]\end{cases} \tag{37}$$

Noticing the matrix dimensions, the system of Eq. (37) is likely to be under-determined to estimate the full set of mount parameters $\mathbf{x}$, i.e. $q\cdot m<(p+n)$. Fortunately the mount parameters in $\mathbf{x}$ are assumed to be invariant of frequency and operational conditions. Hence the conditioning of the problem can be improved by stacking all acquired data vertically, namely for one of the following combinations of dimensions:

- frequency lines $(\omega_1,\ldots,\omega_k)$ and measurement cycles $(1,\ldots,r)$, in case of unprocessed measurement data;
- motor orders and RPM points, if available from post-processing or order analysis.

Stacking all information vertically renders the system of Eq. (37) sufficiently determined to solve for $\mathbf{x}$, for instance in a least-square[20] sense which yields the best fit for all mount parameters. For instance, by stacking all $p+n$ receiver and indicator DoFs, k frequency points and r measurement cycles, the obtained linear system to solve reads

$$\begin{bmatrix}\mathbf{u}^{(1)}_3(\omega_1)\\ \vdots\\ \mathbf{u}^{(r)}_4(\omega_k)\end{bmatrix} = \begin{bmatrix}\mathbf{A}^{(1)}_3(\omega_1)\\ \vdots\\ \mathbf{A}^{(r)}_4(\omega_k)\end{bmatrix}\mathbf{x} \quad\Longrightarrow\quad \mathbf{x}=(\tilde{\mathbf{A}})^{+}\tilde{\mathbf{u}} \tag{38}$$

The mount parameters $\mathbf{x}$ fitted by Eq. (38) can be substituted back into Eq. (35b) to find the mount stiffnesses $\mathbf{z}^{\mathrm{mt}}(\omega)$. These are normally assumed to be independent of the operational conditions and assembly under test, although one may prefer to consider multiple amplitude ranges when the mounts exhibit strong non-linear behaviour.

Operational loads & path contributions: Interface forces can be calculated for each operational test by substituting the estimated mount stiffnesses into Eq. (34b). The interface forces are finally multiplied with their respective FRFs of the passive side to compute the path contributions to the receiver DoFs of interest

$$\mathbf{u}_3=\mathbf{Y}^{\mathrm{B}}_{32}\mathbf{g}^{\mathrm{B}}_2=\mathbf{Y}^{\mathrm{B}}_{32}\left(\mathbf{u}^{\mathrm{A}}_2(\omega)-\mathbf{u}^{\mathrm{B}}_2(\omega)\right)\circ\boldsymbol{\Psi}(\omega)\mathbf{x} \tag{39}$$

Several variants and case studies of OPAX are discussed in [125]. Some special cases are noted here:

- In case that all mount parameters are available a priori, the mount identification steps can be skipped and no indicator DoFs are required. The interface forces can be calculated directly from Eq. (34a) or (34b). This results in the classical mount-stiffness TPA approach as discussed in Section 3.2.2.
- For systems with rigid connections, the differential displacement becomes zero. In other words, displacement compatibility is fully satisfied ($\mathbf{u}^{\mathrm{A}}_2=\mathbf{u}^{\mathrm{B}}_2$), hence Eq. (34a) or (34b) can no longer be used to determine the interface forces. For this case it is suggested in [125] to use the passive-side interface displacement only in combination with a narrow-band mount model

  $$\mathbf{g}^{\mathrm{B}}_2=\mathbf{Z}^{\mathrm{mt}}\mathbf{u}^{\mathrm{B}}_2$$

  If the mount model bandwidth reduces to single frequency lines, this formulation is said to be equivalent to the classical matrix-inverse TPA (see Section 3.2.3), where $\mathbf{Z}^{\mathrm{mt}}$ now represents the impedance of the passive side's interfaces. In fact, to be exactly consistent, $\mathbf{Z}^{\mathrm{mt}}$ should equal $(\mathbf{Y}^{\mathrm{B}}_{22})$ as can be verified by comparing the interface force with Eq. (4). This matrix is generally non-diagonal and operational identification of all its elements can be cumbersome.
- Acoustic loads related to air-borne transmission paths cannot be described by Eq. (34a) or (34b). Each acoustic pressure p_2 (measured near the source) needs to be associated with a single volumetric velocity q_2 at the source structure. These are related through an acoustic impedance z^{air} which is best described using a multi-band model. The total system of

[20] Unit normalisation should be taken into account when responses of different quantities are used.

Table 1
Summary and classification of eleven methods presented in the TPA framework.

Family	Method	Section	Oper. measurement		Source characterisation			Apply to
			Quantity	On system	Quantity		Using	FRFs
Classical	Direct force	3.2.1	$\mathbf{g}_2^{\mathrm{B}}$	AB	Interface force	$\mathbf{g}_2^{\mathrm{B}}$	–	$\mathbf{Y}_{32}^{\mathrm{B}}$
	Mount stiffness	3.2.2	$\mathbf{u}_2^{\mathrm{A}}, \mathbf{u}_2^{\mathrm{B}}$	AB	Interface force	$\mathbf{g}_2^{\mathrm{B}}$	$\mathbf{Z}^{\mathrm{mt}}$	$\mathbf{Y}_{32}^{\mathrm{B}}$
	Matrix inverse	3.2.3	$\mathbf{u}_4$	AB	Interface force	$\mathbf{g}_2^{\mathrm{B}}$	$\mathbf{Y}_{42}^{\mathrm{B}}$	$\mathbf{Y}_{32}^{\mathrm{B}}$
Component based	Blocked force	3.3.2	$\mathbf{g}_2^{\mathrm{b1}}$	A (blocked)	Equiv. force	$\mathbf{f}_2^{\mathrm{eq}}$	–	$\mathbf{Y}_{32}^{\mathrm{AB}}$
	Free velocity	3.3.3	$\mathbf{u}_2^{\mathrm{free}}$	A (free)	Equiv. force	$\mathbf{f}_2^{\mathrm{eq}}$	$\mathbf{Y}_{22}^{\mathrm{A}}$	$\mathbf{Y}_{32}^{\mathrm{AB}}$
	Hybrid interface	3.3.4	$\mathbf{g}_2^{\mathrm{R}}, \mathbf{u}_2$	AR	Equiv. force	$\mathbf{f}_2^{\mathrm{eq}}$	$\mathbf{Y}_{22}^{\mathrm{A}}$	$\mathbf{Y}_{32}^{\mathrm{AB}}$
	in situ	3.3.5	$\mathbf{u}_2(\mathbf{u}_4)$	AR/AB	Equiv. force	$\mathbf{f}_2^{\mathrm{eq}}$	$\mathbf{Y}_{22\ (42)}^{\mathrm{AR/AB}}$	$\mathbf{Y}_{32}^{\mathrm{AB}}$
	Pseudo-forces	3.3.6	$\mathbf{u}_4$	AR/AB	Pseudo-force	$\mathbf{f}_{\mathrm{ps}}$	$\mathbf{Y}_{4\mathrm{ps}}^{\mathrm{AR/AB}}$	$\mathbf{Y}_{3\mathrm{ps}}^{\mathrm{AB}}$
Transmissibility-based	FRF-based	3.4.1	$\mathbf{u}_4$	AB	(Path contrib.)	–	$(\mathbf{Y}_{31}^{\mathrm{AB}}, \mathbf{Y}_{41}^{\mathrm{AB}})$	$\mathbf{T}_{34}$
	OTPA	3.4.2	$\mathbf{u}_3, \mathbf{u}_4$	AB	(Path contrib.)	–	–	$\mathbf{T}_{34}$
	OPAX	3.4.3	$\mathbf{u}_2^{\mathrm{A}}, \mathbf{u}_2^{\mathrm{B}}, \mathbf{u}_4$	AB	Interface force	$\mathbf{g}_2^{\mathrm{B}}$	$\mathbf{Y}_{42}^{\mathrm{B}}$	$\mathbf{Y}_{32}^{\mathrm{B}}$

acoustic load-pressure relations then reads

$$\mathbf{q}_2 = \mathbf{Z}^{\mathrm{air}}\mathbf{p}_2$$

The volumetric velocities $\mathbf{q}_2$ function as acoustic loads; they can be identified together with the structural interface forces $\mathbf{g}_2^{\mathrm{B}}$ by applying Eqs. (36)–(38). Further remarks and guidelines with respect to air-borne transmission paths are provided in Section 4.3.

In summary, OPAX is a versatile method that can be adapted to a wide range of applications and adjusted for either quick troubleshooting or thorough analysis. The classification of the method as a transmissibility-based TPA method is however arguable. At all times, one requires the FRFs of the passive side $\mathbf{Y}_{32}^{\mathrm{B}}$, which puts the method in the family of classical TPA. Also, the interface loads become an intermediate result of the analysis, which is not the case with other transmissibility-based methods. Therefore OPAX can be positioned as an intermediate method, combining advantages from both the classical and the operational TPA genre.

3.5. Summary of TPA methods

In this framework 11 TPA methods have been derived and classified into three families. The global steps required for each family were schematically summarised in Fig. 1. A brief overview of the discussed methodologies is presented in Table 1. All 11 methods prescribe a task of *operational measurement*. Various testing environments can be handled, namely in assembly with the targeted passive structure (AB), on a test rig (AR) or against fixed or free boundary conditions (A). However, as can be observed from Table 1, the chosen test environment and measurement equipment does not necessarily confine the choice of TPA family to be applied.

Let us substantiate this statement with the following example. Suppose one has conducted a series of operational tests on an assembled system AB that had been equipped with receiver DoFs $\mathbf{u}_3$ and indicator DoFs $\mathbf{u}_4$, for instance as depicted in Fig. 3c. Naturally, after demounting the source component and measuring the passive side FRFs $\mathbf{Y}^{\mathrm{B}}$ (for instance from impact measurement interfaces), a *classical matrix-inverse TPA* (Section 3.2.3) can be performed, providing insight in the interface forces and path contributions for the particular assembly.

Alternatively one could choose to measure the assembled system FRFs $\mathbf{Y}^{\mathrm{AB}}$, allowing us to calculate source-specific equivalent forces by the application of the *in situ TPA* method (Section 3.3.5). If the geometry of the assembly prevents proper excitation at the interfaces, one might instead revert to the *pseudo-forces TPA* methodology (Section 3.3.6) and excite alternative points on the source. Still, the same operational response data $\mathbf{u}_4$ can be used here.

However if one runs short of time or motivation, the *Operational TPA* method (Section 3.4.2) would probably be appropriate. Transmissibility can be estimated purely from the available operational response data $(\mathbf{u}_3, \mathbf{u}_4)$, provided that enough independent operational cases were measured. The transmissibility $\mathbf{T}_{34}$ allows us to calculate partial responses corresponding to the indicator DoFs.

As demonstrated, the TPA classification ultimately determines how the source is characterised. The methods pertaining to the family of classical TPA describe the source vibrations for a particular assembly with a passive receiving structure. The component-based approaches depict the source by forces that are a property of the source only. Lastly the methods based on transmissibility skip the stage of source characterisation and only provide information on the source's path contributions.

4. General considerations

Key to conducting a successful TPA is to understand the conceptual basics of the methods applied. However, proper application of experimental techniques is perhaps equally important. This section discusses a couple of practical aspects that

are frequently – but certainly not always – encountered when conducting a TPA. Theoretical derivations have been kept brief; the intention is to address a couple of aspects and provide useful references to related literature.

4.1. Source dependency on mounting conditions

Several component TPA methods propose to perform the operational test in an environment different from the targeted assembly. A crucial assumption herein is that the operational source excitation $\mathbf{f}_1$ is independent of the mounting condition. This dependency only refers to the internal mechanisms creating the excitation $\mathbf{f}_1$. The effect of $\mathbf{f}_1$ on the interface DoFs $\mathbf{u}_2$ is governed by the transfer dynamics, which is correctly accounted for by each method.[21]

The blocked-force and free-velocity methods constitute the two extreme boundary conditions for which the active system can be tested. The hybrid interface method imposes boundary conditions depending on the dynamic stiffness of the test rig. For all three cases, the excitation may thus be influenced by the different mounting stiffness. Note that the in situ and pseudo-forces method both allow us to conduct operational measurement in the target assembly, such that the boundary condition is already the one aimed for.

Some typical sources of excitation and their potential sensitivity to the imposed boundary conditions are discussed below:

- *Rotational orders*: Excitations related to the speed of some rotating system are not expected to be influenced by the boundary conditions. Such excitations are typically identified as orders relative to the RPM, i.e. distinct harmonics in the frequency spectrum with a fixed ratio to the fundamental frequency of the rotational source. Orders arise whenever a periodic excitation is not purely sinusoidal, such as the combustions in an engine, unbalance of a shaft or the torque ripple related to the number of poles in an electric machine.
- *Pre-loading*: Gearing systems are known to be affected by pre-loading. For instance, if the housing of a gearbox is bent, a slight misalignment of the gears can occur which may result in a dramatic increase of the internal excitations. However pre-loading relates to the static mounting condition ($\omega = 0$) rather than the dynamic interaction. As long as the static stiffness of the testing environment is in the same order as the targeted passive system, the influence should be minimal [77].
- *Internal non-linearities*: Vibrations that are caused or influenced by internal non-linearities may be affected by dynamic interaction. Discussion of this topic is beyond the scope of this paper. In general, it is advised to design the mounting structure such that it exhibits similar dynamic behaviour on the interfaces.

If the purpose of study is to investigate the actual influence of the mounting conditions on the excitation, one could for instance turn to hardware-in-the-loop (HiL) testing or real-time substructuring strategies, allowing us to actively adjust the dynamic stiffness at the interfaces [126–128].

4.2. Multiple simultaneous sources

Many products contain multiple sources of vibration that operate simultaneously. To a large extend, these components can be analysed separately and their contributions superimposed. However separate analysis of components is not always possible in practice. Either the components require simultaneous operation for functionality (think of a gearbox driven by an engine), or secondary sources of vibration, not of interest for the analysis, can simply not be deactivated during operational test. In any event, one should pay special attention to make sure that contributions of one source do not spill over into the analysis of the other.

Imagine simultaneous operation of two sources A and A′, as illustrated in Fig. 10. Although $\mathbf{f}_1$ and $\mathbf{f}_{1'}$ may be independent mechanisms, the resulting interface forces $\mathbf{g}_2^{\mathrm{B}}$ and $\mathbf{g}_{2'}^{\mathrm{B}}$ comprise contributions of each other, being intrinsic to the total system ABA′. When the interface forces are measured directly (Section 3.2.1), the responses $\mathbf{u}_3$ (omitted in the figure) follow from simple superposition

$$\mathbf{u}_3 = \mathbf{Y}_{32}^{\mathrm{B}}\mathbf{g}_2^{\mathrm{B}} + \mathbf{Y}_{32'}^{\mathrm{B}}\mathbf{g}_{2'}^{\mathrm{B}} \tag{40}$$

Hence, even when considering the contributions in Eq. (40) individually, effects of other sources are blended in, because the interface forces ($\mathbf{g}_2^{\mathrm{B}}$) contain contributions of the other sources.

A second problem arises when determining interface forces indirectly from measured responses, for instance using the matrix inverse method (Section 3.2.3). Provided that both interfaces are sufficiently monitored by indicator DoFs, i.e. $\mathbf{u}_4$ and $\mathbf{u}_{4'}$, the correct interface forces can be retrieved by solving the following system for $\mathbf{g}_2^{\mathrm{B}}$ and $\mathbf{g}_{2'}^{\mathrm{B}}$:

$$\begin{bmatrix} \mathbf{u}_4 \\ \mathbf{u}_{4'} \end{bmatrix} = \begin{bmatrix} \mathbf{Y}_{42}^{\mathrm{B}} & \mathbf{Y}_{42'}^{\mathrm{B}} \\ \mathbf{Y}_{4'2}^{\mathrm{B}} & \mathbf{Y}_{4'2'}^{\mathrm{B}} \end{bmatrix} \begin{bmatrix} \mathbf{g}_2^{\mathrm{B}} \\ \mathbf{g}_{2'}^{\mathrm{B}} \end{bmatrix} \tag{41}$$

Indeed, the crosstalk is cancelled due to inversion of the fully determined FRF matrix, that was obtained by exciting both interfaces of the *disassembled* receiving subsystem B. However, if the interfaces with source A′ are not instrumented with indicator DoFs $\mathbf{u}_{4'}$

[21] It is arguable whether a vibrating mechanism is best characterised by applied forces or imposed displacements. Both cases are discussed in [82] and it is shown that a displacement source can be implemented with similar ease as an applied force.

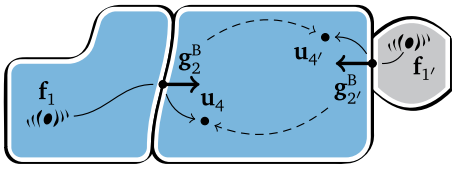

Fig. 10. Multiple vibration sources A (left) and A′ (right) operating simultaneously. The secondary transmission paths are dashed.

(perhaps because a vibration source was not recognised at all), one cannot distinguish the contributions of A from A′. This clearly leads to a contamination of the estimated interface force $\hat{\mathbf{g}}_2^B$ by application of Eq. (10), as only $\mathbf{Y}_{42}^B$ and $\mathbf{u}_4$ are available

$$\hat{\mathbf{g}}_2^B = \left(\mathbf{Y}_{42}^B\right)^+ \mathbf{u}_4 = \mathbf{g}_2^B + \left[\left(\mathbf{Y}_{42}^B\right)^+ \mathbf{Y}_{42'}^B\right]\mathbf{g}_{2'}^B \neq \mathbf{g}_2^B \tag{42}$$

Regarding component-based TPA, the blocked force, free velocity and hybrid interface method are essentially not suited for simultaneous operation, given their particular boundary conditions. For the in situ and pseudo-forces method, a similar reasoning holds as for the classical matrix inverse discussion. FRFs of the fully assembled system ABA′ are required to construct the in situ TPA problem (Section 3.3.5)

$$\begin{bmatrix}\mathbf{u}_4\\ \mathbf{u}_{4'}\end{bmatrix} = \begin{bmatrix}\mathbf{Y}_{42}^{AB} & \mathbf{Y}_{42'}^{AB}\\ \mathbf{Y}_{4'2}^{AB} & \mathbf{Y}_{4'2'}^{AB}\end{bmatrix}\begin{bmatrix}\mathbf{f}_2^{eq}\\ \mathbf{f}_{2'}^{eq}\end{bmatrix} \tag{43}$$

Interestingly, if the problem is properly conditioned, solving of Eq. (43) leads to equivalent forces $\mathbf{f}_2^{eq}$ and $\mathbf{f}_{2'}^{eq}$ that describe the sources independently. After all, the equivalent forces correspond to the theoretical blocked forces measured in separate isolated environments. Therefore, equivalent forces potentially yield a clearer, more distinct characterisation of the separate source contributions than the classical TPA interface forces, which may be noted as an additional benefit of component-based TPA.

With respect to transmissibility-based TPA, sources can only be distinguished in terms of the monitored transition paths [78]. The main problem of neglecting such paths is that vibrations of source A′ appear as contributions coming from source A. This is not easily recognised, as the summed contributions at $\mathbf{u}_3$ would probably match the measured $\mathbf{u}_3$ all the same [117].

In general, when performing tests in an assembled system, results should be interpreted with caution when active systems are present that are not considered in the analysis. Neglecting sources or paths results in incorrect estimation of forces and path contributions by applying matrix inversion. Nevertheless, when all sources are properly monitored, there is no fundamental restriction involved in simultaneous analysis of multiple sources.

4.3. Air-borne transmission paths

An essential question in NVH studies is the relative importance of structure-borne and air-borne paths. If the sound pressure at target locations is predominantly caused by radiation from parts at the passive side (e.g. panels in the interior of a vehicle), one can assume that the transfer problem is mainly of structure-borne nature. After all these parts radiate due to vibrations that are transmitted over the structural interfaces. The relation between acoustic pressure and forces is governed by structural-acoustic FRFs in [Pa/N]. As mentioned in Section 3.1, such response functions can straightforwardly be combined with structural response functions in an FRF matrix, since both types of responses are force-induced.

However when a significant part of the acoustic pressure is related to direct radiation of the source, air-borne paths should be analysed separately. Analogue to structural transfer functions $\mathbf{Y}$, acoustic transfer functions $\mathbf{H}$ describe the responses of acoustic pressures to acoustic loads $\mathbf{q}$, commonly expressed as volume velocities in [m^3/s]. A typical situation is sketched in Fig. 11; the acoustic load generated by the source is denoted by $\mathbf{q}_1$. The combined problem, including both structural and acoustic path contributions, reads

$$\mathbf{p}_3 = \mathbf{Y}_{31}^{AB}\mathbf{f}_1 + \mathbf{H}_{31}^{AB}\mathbf{q}_1 \tag{44}$$

Analysis of air-borne transmission paths is a delicate task that poses many practical challenges. First, a typical sound-radiating source does by no means behave as an ideal mono-pole, meaning that one cannot easily characterise the radiation of the source $\mathbf{q}_1$. Instead one has to surround the source component by a number of "substitute" mono-poles [129,130], representing the spatial distribution of the radiated sound by a finite number of volume velocity DoFs $\mathbf{q}_2$.[22]

A second challenge lies in the measurement of the acoustic transfer paths $\mathbf{H}_{32}^{AB}$. Whereas impact hammers or shakers are very well capable of applying a concentrated force onto a structure, the acoustic counterpart requires excitation by a volume source which is far from trivial. Reciprocal measurement techniques are often used, reducing the required number of acoustic excitations. Theory and applications of reciprocity have been extensively studied, see for instance [83–85,131] and reviews [86,87].

[22] Note that this is conceptually analogue to the structure-borne TPA assumption, namely characterising the unmeasurable source vibrations $\mathbf{f}_1$ by means of forces at the interfaces $\mathbf{g}_2$.

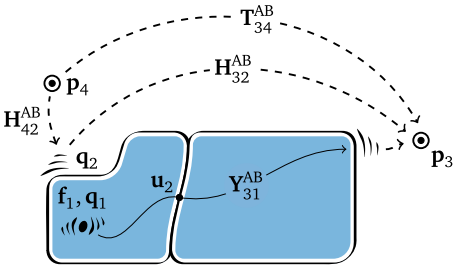

Fig. 11. Various methods to consider air-borne transmission paths related to direct acoustic radiation of the source component.

Finally, not all TPA methods are suitable for air-borne problems in practice. Direct measurement of acoustic loads $\mathbf{q}_2$ has only recently been enabled by means of a directional particle velocity sensing device [132,133] but practical TPA examples are rare [134]. It is more common to determine acoustic loads inversely, for instance from pressure indicator microphones $\mathbf{p}_4$ around the source [135,136] or by the use of advanced imaging techniques such as Near-field Acoustic Holography (NAH) [137–139]. For quick estimation of air-borne path contributions, transmissibility-based methods such as Operational TPA are suitable, avoiding explicit treatment of the acoustic loads. The various concepts are illustrated in Fig. 11 and formulated by Eqs. (45a)–(45c)

$$\mathbf{p}_3 = \mathbf{H}_{32}^{AB}\mathbf{q}_2 \qquad \text{(direct measurement)} \tag{45a}$$

$$\mathbf{p}_3 = \mathbf{H}_{32}^{AB}\mathbf{q}_2 \quad \text{with } \mathbf{q}_2 = \left(\mathbf{H}_{42}^{AB}\right)^{+}\mathbf{p}_4 \qquad \text{(matrix} - \text{inverse)} \tag{45b}$$

$$\mathbf{p}_3 = \mathbf{T}_{34}^{AB}\mathbf{p}_4 \quad \text{with } \mathbf{T}_{34}^{AB} = \mathbf{S}_{34}\mathbf{S}_{44}^{-1} \qquad \text{(operational TPA)} \tag{45c}$$

The operational TPA method, when strictly applied to air-borne path analysis, requires APS and CPS spectra to be calculated from the operational pressure responses $(\mathbf{p}_3, \mathbf{p}_4)$. When combined with structural indicator points $\mathbf{u}_4$, a quick investigation can be made of the proportion between structure-borne and air-borne path contributions [55]. Note that the OPAX method actually implements the matrix-inverse concept of Eq. (45b), with the remark that the acoustical impedance, represented by the term $(\mathbf{H}_{42}^{AB})^{+}$, is parametrised and estimated during operational tests.

Regarding source characterisation in a component-TPA fashion, interesting equivalent source concepts have been explored such as *blocked pressure* and *surface impedance*; see for instance [140–142] and references therein.

4.4. Interface description & rotational DoFs

A crucial factor in TPA is correct and complete description of the interfaces that constitute the transfer paths from active to passive components. It is commonly known that neglecting transfer paths can result in a highly distorted depiction of the transfer problem, especially for TPA methods that employ matrix-inversion techniques [10,117]. So far it has been discussed how the seemingly complex problem of vibration transmission can be analysed using a limited number of transfer functions and corresponding forcing degrees of freedom. These DoFs must however be sufficient to model the behaviour of the interface in full.

Interface modelling is an active research topic in the field of experimental dynamic substructuring and the requirements for TPA are in fact very similar. Some aspects related to interface modelling and rotational DoFs are addressed here.

Rotational DoFs: As rotation sensors and transducers have not been the practical standard over the past,[23] rotational DoFs are in practice often handled indirectly, e.g. by means of multiple translational DoFs at certain distances from each other [146,147]. Simple finite difference approaches such as $\theta = (u_0 - u_d)/d$ may suffice for simple plate or beam problems [148,149], but do not provide full 6-DoF kinematics needed to model all translational and rotational transmission paths.

More promising approaches [150,151] employ a kinematic mapping matrix $\mathbf{R}$ that relates $n > 6$ translational displacements $\mathbf{u}$ to 6 generalised coordinates $\tilde{\mathbf{u}}$ per connection point. This assumes local rigid behaviour of the interface, which can be described by 3 translations and 3 rotations. When the DoFs $\mathbf{u}$ are properly positioned and oriented, a pseudo-inverse $\mathbf{R}^{+}$ exists that linearly transforms the original measurement data to collocated 6-DoF information. An analogue approach exists for the mapping of $m > 6$ translational forces. Collocated 6-DoF FRFs $\tilde{\mathbf{Y}}$ are obtained by applying both transformations sequentially to the measured FRF matrix $\mathbf{Y}$. A summary based on [152] is presented here

$$\begin{cases} \mathbf{u} = \mathbf{R}\tilde{\mathbf{u}} \\ \tilde{\mathbf{u}} = \mathbf{R}^{+}\mathbf{u} \end{cases} \quad \text{with } \mathbf{R} \in \mathbb{R}^{n\times 6} \qquad \begin{cases} \tilde{\mathbf{f}} = \mathbf{G}\mathbf{f} \\ \mathbf{f} = \mathbf{G}^{+}\tilde{\mathbf{f}} \end{cases} \quad \text{with } \mathbf{G} \in \mathbb{R}^{m\times 6} \qquad \begin{cases} \mathbf{u} = \mathbf{Y}\mathbf{f} \\ \tilde{\mathbf{u}} = \tilde{\mathbf{Y}}\tilde{\mathbf{f}} \end{cases} \quad \text{with } \tilde{\mathbf{Y}} = \mathbf{R}^{+}\mathbf{Y}\mathbf{G}^{+} \in \mathbb{R}^{6\times 6}$$

Transformation to a so-called *virtual point* has some additional advantages. First, the virtual point can be positioned freely, such that it can be made compatible with the interfaces of the connected subsystems, possibly obtained from FE modelling. Secondly, by monitoring the residual of the transformation, a quantitative value can be obtained for the consistency of the

[23] Some examples of unconventional hardware for rotation measurement or excitation can be found in [143–145].

measured data and "rigidness" of the motion around the interface. Regarding virtual point FRFs, reciprocity can be evaluated since the virtual motion and loads are concentrated in the virtual point. Lastly, driving-point FRFs can be obtained without actually exciting onto or in line with the sensors, as the transformation matrix for displacements and forces may be different. Details on the virtual point transformation and applications to substructuring and TPA are discussed in [101,152,153].

Inverse determination of rotational forces: Several TPA techniques rely on matrix-inverse force determination schemes. If the application requires to describe both translational and rotational transmission, 6 forces per connection point are to be determined. Nevertheless, one can retain the original FRFs for translational motion $\mathbf{u}_4$ and employ virtual point mapping for the forces only. Let us illustrate this for the case of interface force determination, based on Eq. (10)

$$\tilde{\mathbf{g}}_2^{\mathrm{B}} = \left(\mathbf{Y}_{42}^{\mathrm{B}}\mathbf{G}_2^{+}\right)^{+}\mathbf{u}_4$$

The part between the brackets forms the admittance FRFs relating the set of 6 virtual-point interface forces and moments $\tilde{\mathbf{g}}_2^{\mathrm{B}}$ to translational indicator DoFs $\mathbf{u}_4$. The fundamental condition here is that the full set of interface loads $\tilde{\mathbf{g}}_2^{\mathrm{B}}$ is *observable* from the set of indicator DoFs $\mathbf{u}_4$.[24]

Continuous interfaces: Not all interface problems can be properly described by a small number of connection points. Some systems (such as the interface between gearbox and engine of a vehicle or turbine blades and hub of a wind turbine) comprise larger connecting surfaces, flanges or patterns of closely spaced bolts. Hence, simplification of connectivity is no longer acceptable and the trivial 6 rigid interface modes need to be augmented by a number of flexible modes, which are not naturally obtained from measurement. Information from static FEM analysis can be used to extrapolate the measured points, for instance using the System Equivalent Reduction Expansion Process (SEREP) [154]. Another interesting concept is the temporary attachment of a flexible fixture, allowing us to better measure and/or excite the rotational and flexible modes of a subsystem [155]. This concept, better known as the *transmission simulator*, has recently gained popularity in the field of dynamic substructuring [156]. Applications to TPA have not yet been reported; however the decoupling techniques involved [106,157] are related to inverse source characterisation ideas as seen in e.g. the in situ method.

4.5. Evaluation of paths contributions

The set of receiver responses $\mathbf{u}_3$ are in this framework often considered as the end result of a TPA method. However, the actual purpose of a TPA is rather to identify the individual contributions that sum up to these responses, because these contributions reveal the amount of vibrations transmitted through each path. Transfer path contributions can be evaluated in various ways; the most common methods are summarised here:

- *Partial responses*: Receiver response spectra are composed from the complex sum of the partial response spectra, i.e. the sum of all contributions over the considered transfer paths. To illustrate for classical TPA Eq. (6) the p receiver response spectra u_i are composed from their m path contributions as follows:

$$u_{i,j}(\omega) = Y_{ij}^{\mathrm{B}}(\omega)g_j^{\mathrm{B}}(\omega) \quad \Longrightarrow \quad u_i(\omega) = \sum_{j=1}^{m} u_{i,j}(\omega) \quad \begin{cases} i \in 1,\ldots,p \\ j \in 1,\ldots,m \end{cases}$$

  Partial responses are obtained for all three families and can thus be used to compare the results of various methods. They are typically visualised in 3D images with frequency ω on one axis and the m path contributions on the other axis. Such graphics allow for quick visual troubleshooting of the dominant transfer paths and critical frequency ranges. Other typical diagrams derived from partial responses include Campbell plots, nth-octave plots, engine order plots, phase vector plots and sum levels over RPM; see for instance the graphics in [9–11,120].
- *Power flow*: Power flow investigations are used for instance to determine the activity of the source, localise energy concentrations or quantify damping over the interfaces [89,158–160]. Complex power is commonly expressed as the conjugated product of force and velocity spectra, which can be related to AC current and voltage in electrical engineering. As velocity is a result of force times mobility (i.e. velocity FRF, denoted by $\dot{\mathbf{Y}}$), the phase of the power flow is directly related to the phase of the mobility FRFs

$$\mathcal{P} = \tfrac{1}{2}\mathbf{f}^H\dot{\mathbf{u}} = \tfrac{1}{2}\mathbf{f}^H\dot{\mathbf{Y}}\mathbf{f}$$

  When considered for interface DoFs, the real part of $\mathcal{P}$ represents the dissipated power over the interfaces whereas the imaginary part quantifies the dynamic interaction between the components. As separate knowledge of forces and motion is required, transmissibility-based methods are not suitable for power flow analysis.
- *Auralisation*: Auralisation is time-domain evaluation of path contributions by means of audible sound [161]. Some commercial packages offer the possibility to listen to partial responses, but the implementation often remains proprietary. In many cases, the essential TPA calculations are performed in the frequency domain. The outputs of the

[24] Transmissibility-based techniques also benefit from double instrumentation along transmission paths, e.g. two tri-axial accelerometers close to each other. Although rotational moments are not explicitly being characterised, it can be reasoned that the *effects* are better observable from the increased set of indicator DoFs $\mathbf{u}_4$, leading to a more truthful reconstruction of the target responses.

analysis, e.g. receiver responses $\mathbf{u}_3(t)$, are ultimately calculated in the time domain, for instance using approximated FIR filter banks or by convolution with Impulse Response Functions (IRFs)[25]

$$\mathbf{u}_3(t) = \int_0^t \mathbf{Y}_{32}^{\mathrm{B}}(t-\tau)\mathbf{g}_2^{\mathrm{B}}(\tau)\, d\tau$$

Some methods are specifically formulated for time-domain operation, such as the classical TPA force reconstruction algorithms as proposed by [38,95]. For the purpose of component-based TPA, an interesting blocked-force reconstruction technique was developed by Sturm et al. [111,112] based on the in situ TPA concept. This method is essentially a modification of the Least Mean Square (LMS) algorithm and is inverse-free. Time-domain variants of operational TPA are often referred to as Transfer Path Synthesis (TPS) [123] or time-domain Independent Component Analysis (time-domain ICA) [164].

5. Conclusions

This paper presents a systematic derivation of several methods to analyse vibration transmission problems, together defining a large part of the landscape of Transfer Path Analysis. The evolution of TPA has been discussed, from early theoretical developments to practical TPA methods. A general framework for the derivation of TPA methods has been presented, proposing a classification into the families of classical, component-based and transmissibility-based TPA. The classification defines the principle of source characterisation, but does not necessarily prescribe the environment for operational testing. It was emphasised that the three families are highly interrelated and that similar accuracy can be reached, provided that the theoretical assumptions are properly transposed to application. Common practicalities have been discussed, such as superposition of sources in a system, analysis of air-borne paths and measurement of rotational DoFs. Altogether this paper could be a useful asset to help understanding the countless possibilities and combinations within the TPA paradigm.

At present, little has been suggested about the methods' relative success for typical industrial cases and sensitivity to various sources of error. Further research, in both numerical simulation and experimental validation, would substantiate this TPA framework in that respect.

Appendix A. Transfer dynamics in the context of LM-FBS

The methodology of Frequency Based Substructuring (FBS) provides us with means to conveniently compute assembled FRFs for an arbitrary number of subsystems [13]. The transfer problem in this framework is limited to an assembly of only two subsystems: the first containing the excitation and the second the receiving responses. Still, this problem is representative for a large range of TPA applications. Note that the task of source characterisation is normally not considered part of substructuring; guidelines are proposed in [82].

Let us examine how this problem can be expressed from application of Lagrange-Multiplier Frequency Based Substructuring. LM-FBS prescribes the following three-field formulation, similar to Eqs. (2) and (3):

$$\mathbf{u} = \mathbf{Y}(\mathbf{f}+\mathbf{g}); \quad \mathbf{B}\mathbf{u} = \mathbf{0}; \quad \mathbf{g} = -\mathbf{B}^T\boldsymbol{\lambda}$$

which leads to the general equation for the dually assembled system

$$\mathbf{u} = \mathbf{Y}\mathbf{f} - \mathbf{Y}\mathbf{B}^T\left(\mathbf{B}\mathbf{Y}\mathbf{B}^T\right)^{-1}\mathbf{B}\mathbf{Y}\mathbf{f} \tag{A.1}$$

Note that the set of interface forces $\mathbf{g}$ was eliminated by enforcing coordinate compatibility and force equilibrium. For the TPA example as discussed in this framework, the vectorised terms can be defined as follows:

$$\mathbf{Y} \triangleq \begin{bmatrix} \mathbf{Y}_{11}^{\mathrm{A}} & \mathbf{Y}_{12}^{\mathrm{A}} & \mathbf{0} & \mathbf{0} & \mathbf{0} \\ \mathbf{Y}_{21}^{\mathrm{A}} & \mathbf{Y}_{21}^{\mathrm{A}} & \mathbf{0} & \mathbf{0} & \mathbf{0} \\ \mathbf{0} & \mathbf{0} & \mathbf{Y}_{22}^{\mathrm{B}} & \mathbf{Y}_{23}^{\mathrm{B}} & \mathbf{Y}_{24}^{\mathrm{B}} \\ \mathbf{0} & \mathbf{0} & \mathbf{Y}_{32}^{\mathrm{B}} & \mathbf{Y}_{33}^{\mathrm{B}} & \mathbf{Y}_{34}^{\mathrm{B}} \\ \mathbf{0} & \mathbf{0} & \mathbf{Y}_{42}^{\mathrm{B}} & \mathbf{Y}_{43}^{\mathrm{B}} & \mathbf{Y}_{44}^{\mathrm{B}} \end{bmatrix}; \quad \mathbf{u} \triangleq \begin{bmatrix} \mathbf{u}_1 \\ \mathbf{u}_2^{\mathrm{A}} \\ \mathbf{u}_2^{\mathrm{B}} \\ \mathbf{u}_3 \\ \mathbf{u}_4 \end{bmatrix}; \quad \mathbf{f} \triangleq \begin{bmatrix} \mathbf{f}_1 \\ \mathbf{0} \\ \mathbf{0} \\ \mathbf{0} \\ \mathbf{0} \end{bmatrix}; \quad \mathbf{B} \triangleq \begin{bmatrix} \mathbf{0} & -\mathbf{I} & \mathbf{I} & \mathbf{0} & \mathbf{0} \end{bmatrix}$$

[25] Computation of structural responses by convolution of IRFs of substructures relates to the field of Impulse Based Substructuring (IBS) [162,163], which solves the interface problem in the time-domain.

This simplifies the composition of all responses considerably as forces are only applied at the source DoFs of subsystem A. The combined responses read

$$\underbrace{\begin{bmatrix}\mathbf{u}_1\\ \mathbf{u}_2^{\mathrm{A}}\\ \mathbf{u}_2^{\mathrm{B}}\\ \mathbf{u}_3\\ \mathbf{u}_4\end{bmatrix}}_{\mathbf{u}} = \underbrace{\begin{bmatrix}\mathbf{Y}_{11}^{\mathrm{A}}\\ \mathbf{Y}_{21}^{\mathrm{A}}\\ 0\\ 0\\ 0\end{bmatrix}}_{\mathbf{y_f}}\mathbf{f}_1 - \underbrace{\begin{bmatrix}-\mathbf{Y}_{12}^{\mathrm{A}}\\ -\mathbf{Y}_{22}^{\mathrm{A}}\\ \mathbf{Y}_{22}^{\mathrm{B}}\\ \mathbf{Y}_{32}^{\mathrm{B}}\\ \mathbf{Y}_{42}^{\mathrm{B}}\end{bmatrix}}_{\mathbf{YB}^T}\underbrace{\left(\mathbf{Y}_{22}^{\mathrm{A}}+\mathbf{Y}_{22}^{\mathrm{B}}\right)^{-1}}_{(\mathbf{BYB}^T)^{-1}}\underbrace{\left(-\mathbf{Y}_{21}^{\mathrm{A}}\,\mathbf{f}_1\right)}_{\mathbf{YBf}} \tag{A.2}$$

Based on Eq. (A.2), two different forms can be distinguished, namely the responses at the side of respectively subsystem A and subsystem B. The first includes the direct response to the excitation (the term **Yf**), such that an assembled response reads

$$\mathbf{u}_a = \mathbf{Y}_{a1}^{\mathrm{AB}}\mathbf{f}_1 = \mathbf{Y}_{a1}^{\mathrm{A}}\mathbf{f}_1 - \mathbf{Y}_{a2}^{\mathrm{A}}\left(\mathbf{Y}_{22}^{\mathrm{A}}+\mathbf{Y}_{22}^{\mathrm{B}}\right)^{-1}\mathbf{Y}_{21}^{\mathrm{A}}\mathbf{f}_1 \quad \text{for} \quad \mathbf{u}_a \in (\mathbf{u}_1, \mathbf{u}_2^{\mathrm{A}})$$

For subsystem B, the responses are only due to the vibrations that are transferred over the interface. Consequently one obtains for a passive-side response

$$\mathbf{u}_b = \mathbf{Y}_{b1}^{\mathrm{AB}}\mathbf{f}_1 = \mathbf{0} + \mathbf{Y}_{b2}^{\mathrm{B}}\left(\mathbf{Y}_{22}^{\mathrm{A}}+\mathbf{Y}_{22}^{\mathrm{B}}\right)^{-1}\mathbf{Y}_{21}^{\mathrm{A}}\mathbf{f}_1 \quad \text{for} \quad \mathbf{u}_b \in (\mathbf{u}_2^{\mathrm{B}}, \mathbf{u}_3, \mathbf{u}_4)$$

This difference has profound implications with respect to the equivalent source properties in the component-based TPA methods, as was discussed in Section 3.3.

References

[1] M. Harrison, A.O. Sykes, M. Martin, Wave effects in isolation mounts, J. Acoust. Soc. Am. 24 (1) (1952) 62–71, http://dx.doi.org/10.1121/1.1906850.
[2] E. Ungar, C. Dietrich, High-frequency vibration isolation, J. Sound Vib. 4 (2) (1966) 224–241, http://dx.doi.org/10.1016/0022-460X(66)90123-4.
[3] R. Plunkett, Interaction between a vibratory machine and its foundation, Noise Control 4 (1) (1958) 18–22.
[4] J. Soliman, M. Hallam, Vibration isolation between non-rigid machines and non-rigid foundations, J. Sound Vib. 8 (2) (1968) 329–351, http://dx.doi.org/10.1016/0022-460X(68)90236-8.
[5] J.C. Snowdon, Vibration isolation: use and characterization, J. Acoust. Soc. Am. 66 (5) (1979) 1245–1274, http://dx.doi.org/10.1121/1.383546.
[6] R.L. Bisplinghoff, H. Ashley, R.L. Halfman, Aeroelasticity, Addison-Wesley Publishing Company, Cambridge, MA, 1955.
[7] F.J. On, Mechanical Impedance Analysis for Lumped Parameter Multi-degree of Freedom/Multi-dimensional Systems, Technical Report, NASA Technical Note D 3865, 1967.
[8] F. Penne, Shaping the sound of the next-generation BMW, In: Proceedings of the International Conference on Noise and Vibration Engineering (ISMA), Leuven, Belgium, 2004, pp. 25–39.
[9] J. Plunt, Finding and fixing vehicle NVH problems with transfer path analysis, Sound Vib. 39 (11) (2005) 12–16.
[10] H. van der Auweraer, P. Mas, S. Dom, A. Vecchio, K. Janssens, P. van de Ponseele, Transfer Path Analysis in the Critical Path of Vehicle Refinement: The Role of Fast, Hybrid and Operational Path Analysis, Technical Report 2007-01-2352, SAE Technical Paper, 2007, http://dx.doi.org/10.4271/2007-01-2352.
[11] P. Zeller, Handbuch Fahrzeugakustik, Vieweg+Teubner, Wiesbaden, 2009 http://dx.doi.org/10.1007/978-3-8348-8657-6.
[12] G. Cerrato, Automotive sound quality—powertrain, road and wind noise, Sound Vib. 43 (4) (2009) 16–24.
[13] D. de Klerk, D.J. Rixen, S.N. Voormeeren, General framework for dynamic substructuring: history, review and classification of techniques, AIAA J. 46 (8) (2008) 1169–1181, http://dx.doi.org/10.2514/1.33274.
[14] G. R. Kirchhoff, Electricität und magnetismus, in: M. Plank (Ed.), Vorlesungen über mathematische Physik, vol. 3, 1891.
[15] O. Heaviside, Electrical Papers, vols. 1–2, Macmillan, London, pp. 1882–1884.
[16] M.L. Thévenin, Sur un nouveau théoreme d'électricité dynamique [on a new theorem of dynamic electricity], C. R. hebds Séanc. Acad. Sci. 97 (1883) 159–161.
[17] E.L. Norton, Design of Finite Networks for Uniform Frequency Characteristic, Technical Report, Technical Report TM26-0-1860, Bell Laboratories, 1926.
[18] H.L.F. Von Helmholtz, II. Über einige Gesetze der Verteilung elektrischer Ströme in körperlichen Leitern mit Anwendung aug die thierisch-elektrischen Versuche [Some laws concerning the distribution of electrical currents in conductors with applications to experiments on animal electricity], Ann. Phys. Chem. 89 (6) (1853) 211–233.
[19] D.H. Johnson, Origins of the equivalent circuit concept: the voltage–source equivalent, Proc. IEEE 91(4) (2003) 636–640, http://dx.doi.org/10.1109/JPROC.2003.811716.
[20] D.H. Johnson, Origins of the equivalent circuit concept: the current–source equivalent, Proc. IEEE 91(5) (2003) 817–821, http://dx.doi.org/10.1109/JPROC.2003.811795.
[21] P. Gardonio, M. Brennan, On the origins and development of mobility and impedance methods in structural dynamics, J. Sound Vib. 249 (3) (2002) 557–573, http://dx.doi.org/10.1006/jsvi.2001.3879.
[22] A.G. Webster, Acoustical impedance and the theory of horns and of the phonograph, Proc. Natl. Acad. Sci. USA 5(7) (1919) 275 (submitted in 1914).
[23] F.A. Firestone, A new analogy between mechanical and electrical systems, J. Acoust. Soc. Am. 4 (3) (1933) 249–267, http://dx.doi.org/10.1121/1.1901958.
[24] G.J. O'Hara, Mechanical impedance and mobility concepts, J. Acoust. Soc. Am. 41 (5) (1967) 1180–1184, http://dx.doi.org/10.1121/1.1910456.
[25] P. Gardonio, M. Brennan, Mobility and Impedance Methods in Structural Dynamics: An Historical Review, Technical Report, Institute of Sound and Vibration Research (ISVR), University of Southampton, 2000.
[26] F.A. Firestone, Thixt earth and sky with rod and tube; the mobility and classical impedance analogies, J. Acoust. Soc. Am. 28 (6) (1956) 1117–1153, http://dx.doi.org/10.1121/1.1908575.
[27] E.L. Hixson, Mechanical impedance and mobility, in: C.M. Harris, C.E. Crede (Eds.), Shock and Vibration Handbook, 1st ed. McGraw-Hill, New York, 1961, pp. 1–59. (Chapter 10).
[28] A.O. Sykes, Application of admittance and impedance concepts in the synthesis of vibrating systems, In: V. Neubert, J. Raney (Eds.), Synthesis of Vibrating Systems: (Colloquium) Winter Annual Meeting of the ASME, Washington, DC, Shock and Vibration Committee of the Applied Mechanics Division, American Society of Mechanical Engineers, New York, 1971, pp. 22–33.
[29] L. Cremer, M. Heckl, E.E. Ungar, Structure-Borne Sound, 1st ed., Springer, Berlin, Heidelberg, 1973, http://dx.doi.org/10.1007/978-3-662-10118-6.

[30] J. Snowdon, Mechanical four-pole parameters and their application, J. Sound Vib. 15 (3) (1971) 307–323, http://dx.doi.org/10.1016/0022-460X(71)90427-5.
[31] J.S. Bendat, A.G. Piersol, Random Data: Analysis and Measurement Procedures, John Wiley and Sons, Inc., New York, 1971.
[32] J.S. Bendat, A.G. Piersol, Engineering Applications of Correlation and Spectral Analysis, John Wiley & Sons, Inc., New York, London, Sydney, 1980.
[33] J.S. Bendat, Solutions for the multiple input/output problem, J. Sound Vib. 44 (3) (1976) 311–325, http://dx.doi.org/10.1016/0022-460X(76)90504-6.
[34] J.S. Bendat, System identification from multiple input/output data, J. Sound Vib. 49 (3) (1976) 293–308, http://dx.doi.org/10.1016/0022-460X(76)90422-3.
[35] D.J. Ewins, Modal Testing: Theory, Practice and Application, 2nd ed., John Wiley & Sons, Inc., New York, London, Sydney, 2000.
[36] J.W. Verheij, Measuring sound transfer through resilient mountings for separate excitation with orthogonal translations and rotations, In: InterNoise80, Miami, FL, Number 2 in INTER-NOISE and NOISE-CON Congress and Conference Proceedings, Institute of Noise Control Engineering, Washington, 1980, pp. 723–726.
[37] J.W. Verheij, Multi-path sound transfer from resiliently mounted shipboard machinery: experimental methods for analyzing and improving noise control (Ph.D. thesis), Delft University of Technology, The Netherlands, 1982.
[38] R.E. Powell, W. Seering, Multichannel structural inverse filtering, J. Vib. Acoust. 106 (1) (1984) 22–28, http://dx.doi.org/10.1115/1.3269147.
[39] B.J. Dobson, E. Rider, A review of the indirect calculation of excitation forces from measured structural response data, Proc. Inst. Mech. Eng. Part C: J. Mech. Eng. Sci. 204(2) (1990) 69–75, http://dx.doi.org/10.1243/PIME_PROC_1990_204_080_02.
[40] A.N. Thite, D.J. Thompson, The quantification of structure-borne transmission paths by inverse methods. Part 1: improved singular value rejection methods, J. Sound Vib. 264 (2) (2003) 411–431, http://dx.doi.org/10.1016/S0022-460X(02)01202-6.
[41] A.N. Thite, D.J. Thompson, The quantification of structure-borne transmission paths by inverse methods. Part 2: use of regularization techniques, J. Sound Vib. 264 (2) (2003) 433–451, http://dx.doi.org/10.1016/S0022-460X(02)01203-8.
[42] F.X. Magrans, Method of measuring transmission paths, J. Sound Vib. 74 (3) (1981) 321–330, http://dx.doi.org/10.1016/0022-460X(81)90302-3.
[43] O. Guasch, F.X. Magrans, The global transfer direct transfer method applied to a finite simply supported elastic beam, J. Sound Vib. 276 (1) (2004) 335–359, http://dx.doi.org/10.1016/j.jsv.2003.07.032.
[44] O. Guasch, Direct transfer functions and path blocking in a discrete mechanical system, J. Sound Vib. 321 (3) (2009) 854–874, http://dx.doi.org/10.1016/j.jsv.2008.10.006.
[45] O. Guasch, C. García, J. Jové, P. Artís, Experimental validation of the direct transmissibility approach to classical transfer path analysis on a mechanical setup, Mech. Syst. Signal Process. 37 (1) (2013) 353–369, http://dx.doi.org/10.1016/j.ymssp.2013.01.006.
[46] F.X. Magrans, P.V. Rodriguez, G.C. Cousin, Low and mid-high frequency advanced transmission path analysis, In: Proceedings of the XII International Congress on Sound and Vibration (ICSV), Lisbon, Portugal, 2005.
[47] W. Liu, D.J. Ewins, Transmissibility properties of mdof systems, In: Proceedings of the XVI International Modal Analysis Conference (IMAC), Santa Barbara, CA, Society for Experimental Mechanics, Bethel, CT, 1998, pp. 847–854.
[48] P.S. Varoto, K.G. McConnell, Single point vs. multi point acceleration transmissibility concepts in vibration testing, In: Proceedings of the XVI International Modal Analysis Conference (IMAC), Santa Barbara, CA, vol. 1, Society for Experimental Mechanics, Bethel, CT, 1998, pp. 83–90.
[49] A.M.R. Ribeiro, N.M.M. Maia, J.M.M. Silva, Experimental evaluation of the transmissibility matrix, In: Proceedings of the XVII International Modal Analysis Conference (IMAC), Kissimmee, FL, 1999.
[50] A.M.R. Ribeiro, J.M.M. Silva, N.M.M. Maia, On the generalisation of the transmissibility concept, Mech. Syst. Signal Process. 14 (1) (2000) 29–35, http://dx.doi.org/10.1006/mssp.1999.1268.
[51] N.M.M. Maia, J.M.M. Silva, A.M.R. Ribeiro, The transmissibility concept in multi-degree systems, Mech. Syst. Signal Process. 15 (1) (2001) 129–137, http://dx.doi.org/10.1006/mssp.2000.1356.
[52] M. Fontul, A.M.R. Ribeiro, J.M.M. Silva, N.M.M. Maia, Transmissibility matrix in harmonic and random processes, Shock Vib. 11 (5–6) (2004) 563–571, http://dx.doi.org/10.1155/2004/438986.
[53] K. Noumura, J. Yoshida, A method of transfer path analysis for vehicle interior sound with no excitation experiment, In: Proceedings of FISITA 2006 World Automotive Congress, F2006D183, JSAE, 2006.
[54] M. Lohrmann, Operational transfer path analysis: comparison with conventional methods, J. Acoust. Soc. Am. 123 (2008) 3534, http://dx.doi.org/10.1121/1.2934496.
[55] D. de Klerk, A. Ossipov, Operational transfer path analysis: theory, guidelines and tire noise application, Mech. Syst. Signal Process. 24(7) (2010) 1950–1962, Special Issue: ISMA 2010, http://dx.doi.org/10.1016/j.ymssp.2010.05.009.
[56] P. Gajdatsy, K. Janssens, W. Desmet, H. van der Auweraer, Application of the transmissibility concept in transfer path analysis, Mech. Syst. Signal Process. 24 (7) (2010) 1963–1976, http://dx.doi.org/10.1016/j.ymssp.2010.05.008.
[57] J. Scheuren, M. Lohrmann, Transfer path analysis—experiences, expectations and perspectives, In: International Noise and Vibration Colloquium, SAE Brazil, 2014.
[58] J.M. Mondot, B.A.T. Petersson, Characterization of structure-borne sound sources: the source descriptor and the coupling function, J. Sound Vib. 114 (3) (1987) 507–518, http://dx.doi.org/10.1016/S0022-460X(87)80020-2.
[59] B.A.T. Petersson, B.M. Gibbs, Use of the source descriptor concept in studies of multi-point and multi-directional vibrational sources, J. Sound Vib. 168 (1) (1993) 157–176, http://dx.doi.org/10.1006/jsvi.1993.1367.
[60] B.A.T. Petersson, B.M. Gibbs, Towards a structure-borne sound source characterization, Appl. Acoust. 61 (3) (2000) 325–343.
[61] A.T. Moorhouse, On the characteristic power of structure-borne sound sources, J. Sound Vib. 248 (3) (2001) 441–459, http://dx.doi.org/10.1006/jsvi.2001.3797.
[62] A.S. Elliott, A.T. Moorhouse, Characterisation of structure borne sound sources from measurement in-situ, J. Acoust. Soc. Am. 123 (5) (2008) 3176, http://dx.doi.org/10.1121/1.2933261.
[63] A.T. Moorhouse, A.S. Elliott, T.A. Evans, in situ measurement of the blocked force of structure-borne sound sources, J. Sound Vib. 325 (4-5) (2009) 679–685, http://dx.doi.org/10.1016/j.jsv.2009.04.035.
[64] M.H.A. Janssens, J.W. Verheij, D.J. Thompson, The use of an equivalent forces method for the experimental quantification of structural sound transmission in ships, J. Sound Vib. 226 (2) (1999) 305–328, http://dx.doi.org/10.1006/jsvi.1999.2303.
[65] M.H.A. Janssens, J.W. Verheij, A pseudo-forces methodology to be used in characterization of structure-borne sound sources, Appl. Acoust. 61 (3) (2000) 285–308, http://dx.doi.org/10.1016/S0003-682X(00)00035-9.
[66] W.C. Hurty, Vibrations of structural systems by component mode synthesis, J. Eng. Mech. Div. 86 (4) (1960) 51–70.
[67] G.M.L. Gladwell, Branch mode analysis of vibrating systems, J. Sound Vib. 1 (1) (1964) 41–59, http://dx.doi.org/10.1016/0022-460X(64)90006-9.
[68] R.R.J. Craig, M.C.C. Bampton, Coupling of substructures using component mode synthesis, AIAA J. 6 (7) (1968) 1313–1319, http://dx.doi.org/10.2514/3.2947.
[69] S. Rubin, Transmission matrices for vibration and their relation to admittance and impedance, J. Manuf. Sci. Eng. 86 (1) (1964) 9–21, http://dx.doi.org/10.1115/1.3670463.
[70] S. Rubin, Mechanical immittance- and transmission-matrix concepts, J. Acoust. Soc. Am. 41 (5) (1967) 1171–1179, http://dx.doi.org/10.1121/1.1910455.
[71] S. Rubin, Improved component-mode representation for structural dynamic analysis, AIAA J. 13 (8) (1975) 995–1006, http://dx.doi.org/10.2514/3.60497.
[72] B. Jetmundsen, R. Bielawa, W.G. Flannelly, Generalized frequency domain substructure synthesis, J. Am. Helicopter Soc. 33 (1) (1988) 55–64, http://dx.doi.org/10.4050/JAHS.33.55.
[73] J.R. Crowley, A.L. Klosterman, G.T. Rocklin, H. Vold, Direct structural modification using frequency response functions, In: Proceedings of the II International Modal Analysis Conference (IMAC), Orlando, FL, 1984, pp. 58–65.

[74] D. de Klerk, D. Rixen, J. de Jong, The frequency based substructuring method reformulated according to the dual domain decomposition method, In: Proceedings of the XXIV International Modal Analysis Conference (IMAC), St. Louis, MO, Society for Experimental Mechanics, Bethel, CT, 2006.
[75] J. Plunt, E. Kamph, D. Fothergill, Dynamic Analysis and Acoustic Optimization of the Volvo Multi-link Rear Suspension, Technical Paper 891142, SAE International, 1989, http://dx.doi.org/10.4271/891142.
[76] J. Plunt, Examples of Using Transfer Path Analysis (TPA) Together with CAE-Models to Diagnose and Find Solutions for NVH Problems Late in the Vehicle Development Process, Technical Report 2005-01-2508, SAE Technical Paper, 2005, http://dx.doi.org/10.4271/2005-01-2508.
[77] D. de Klerk, Dynamic response characterization of complex systems through operational identification and dynamic substructuring (Ph.D. thesis), Delft University of Technology, The Netherlands, 2009.
[78] D. de Klerk, D.J. Rixen, Component transfer path analysis method with compensation for test bench dynamics, Mech. Syst. Signal Process. 24 (6) (2010) 1693–1710, http://dx.doi.org/10.1016/j.ymssp.2010.01.006.
[79] ISO Technical Committee 43/Subcommittee 1/Workgroup 22 (ISO/TC43/SC1/WG22), Acoustics—Estimation of Airborne Noise Emitted by Machinery Using Vibration Measurement, ISO 7849, International Standards Organisation, 1987.
[80] ISO Technical Committee 43/Subcommittee 1/Workgroup 22 (ISO/TC43/SC1/WG22), Acoustics—Characterization of Sources of Structure-Borne Sound with Respect to Sound Radiation from Connected Structures—Measurement of Velocity at the Contact Points of Machinery when Resiliently Mounted, ISO 9611, International Standards Organisation, 1996.
[81] T. ten Wolde, G.R. Gadefelt, Development of standard measurement methods for structureborne sound emission, Noise Control Eng. J. 28 (1) (1987) 5–14, http://dx.doi.org/10.3397/1.2827676.
[82] D.J. Rixen, A. Boogaard, M.V. van der Seijs, G. van Schothorst, T. van der Poel, Vibration source description in substructuring: a theoretical depiction, Mech. Syst. Signal Process. 60–61 (2015) 498–511, http://dx.doi.org/10.1016/j.ymssp.2015.01.024.
[83] T. ten Wolde, Reciprocity experiments on the transmission of sound in ships (Ph.D. thesis), Delft University of Technology, The Netherlands, 1973.
[84] T. ten Wolde, J.W. Verheij, H.F. Steenhoek, Reciprocity method for the measurement of mechano-acoustical transfer functions, J. Sound Vib. 42 (1) (1975) 49–55, http://dx.doi.org/10.1016/0022-460X(75)90301-6.
[85] F.J. Fahy, The vibro-acoustic reciprocity principle and applications to noise control, Acta Acust. United Acust. 81 (6) (1995) 544–558.
[86] F.J. Fahy, Some applications of the reciprocity principle in experimental vibroacoustics, Acoust. Phys. 49 (2) (2003) 217–229, http://dx.doi.org/10.1134/1.1560385.
[87] T. ten Wolde, Reciprocity measurements in acoustical and mechano-acoustical systems. Review of theory and applications, Acta Acust. United Acust. 96 (1) (2010) 1–13, http://dx.doi.org/10.3813/AAA.918250.
[88] P. Reuss, B. Zeumer, J. Herrmann, L. Gaul, Consideration of interface damping in dynamic substructuring, In: Topics in Experimental Dynamics Substructuring and Wind Turbine Dynamics, vol. 2, Proceedings of the 30th IMAC, A Conference on Structural Dynamics, Springer, New York, 2012, pp. 81–88 (Chapter 10), http://dx.doi.org/10.1007/978-1-4614-2422-2_10.
[89] E. Barten, M.V. van der Seijs, D. de Klerk, A complex power approach to characterise joints in experimental dynamic substructuring, In: Dynamics of Coupled Structures, vol. 1, Proceedings of the 32nd IMAC, A Conference and Exposition on Structural Dynamics, Springer, New York, 2014, pp. 281–296 (Chapter 27), http://dx.doi.org/10.1007/978-3-319-04501-6_27.
[90] S.N. Voormeeren, Dynamic substructuring methodologies for integrated dynamic analysis of wind turbines (Ph.D. thesis), Delft University of Technology, The Netherlands, 2012, http://dx.doi.org/10.4233/uuid:f45f0548-d5ec-46aa-be7e-7f1c2b57590d.
[91] D.J. Thompson, W.J. van Vliet, J.W. Verheij, Developments of the indirect method for measuring the high frequency dynamic stiffness of resilient elements, J. Sound Vib. 213 (1) (1998) 169–188, http://dx.doi.org/10.1006/jsvi.1998.1492.
[92] A.N. Thite, D.J. Thompson, Selection of response measurement locations to improve inverse force determination, Appl. Acoust. 67 (8) (2006) 797–818, http://dx.doi.org/10.1016/j.apacoust.2006.01.001.
[93] H.G. Choi, A.N. Thite, D.J. Thompson, Comparison of methods for parameter selection in Tikhonov regularization with application to inverse force determination, J. Sound Vib. 304 (3) (2007) 894–917, http://dx.doi.org/10.1016/j.jsv.2007.03.040.
[94] P. Mas, P. Sas, Indirect force identification based upon impedance matrix inversion: a study on statistical and deterministical accuracy, In: Proceedings of the International Conference on Noise and Vibration Engineering (ISMA), Leuven, Belgium, 1994.
[95] D.C. Kammer, Input force reconstruction using a time domain technique, J. Vib. Acoust. 120 (4) (1998) 868–874, http://dx.doi.org/10.1115/1.2893913.
[96] D. Sachse, T. Geluk, T. van Wayenberge, Accuracy of inverse load identification techniques for transfer path analysis, In: Automotive Acoustics Conference 2013, 2nd International ATZ Conference, ATZlive, 2013.
[97] F.L.M. dos Santos, B. Peeters, J. Lau, W. Desmet, L.C.S. Góes, An overview of experimental strain-based modal analysis methods, In: Proceedings of the International Conference on Noise and Vibration Engineering (ISMA), Leuven, Belgium, 2014.
[98] H.A. Bonhoff, The influence and significance of cross-order terms in interface mobilities for structure-borne sound source characterization (Ph.D. thesis), Technische Universität, Berlin, 2010.
[99] A. Gaudin, J.F. Beniguel, Low frequency road noise decomposition at wheel center on an roller bench, In: Acoustics 2012, Société Française d'Acoustique, Nantes, France, 2012.
[100] P.L.C. van der Valk, D.J. Rixen, Substituting internal forces for blocked forces or free interface displacements in substructured simulations, In: Topics in Experimental Dynamic Substructuring, vol. 2, Proceedings of the 31st IMAC, A Conference on Structural Dynamics, Springer, New York, 2014, pp. 77–96 (Chapter 8), http://dx.doi.org/10.1007/978-1-4614-6540-9_8.
[101] D.D. van den Bosch, M.V. van der Seijs, D. de Klerk, Validation of blocked-force Transfer Path Analysis with compensation for test bench dynamics, In: Dynamics of Coupled Structures, vol. 1, Proceedings of the 32nd IMAC, A Conference and Exposition on Structural Dynamics, Springer, New York, 2014, pp. 37–49 (Chapter 4), http://dx.doi.org/10.1007/978-3-319-04501-6_4.
[102] M.V. van der Seijs, E.A. Pasma, D. de Klerk, D.J. Rixen, A robust transfer path analysis method for steering gear vibrations on a test bench, In: Proceedings of the International Conference on Noise and Vibration Engineering (ISMA), Leuven, Belgium, 2014.
[103] G. van Schothorst, M.A. Boogaard, G.W. van der Poel, D.J. Rixen, Analysis of ground vibration transmission in high precision equipment by frequency based substructuring, in: Proceedings of the International Conference on Noise and Vibration Engineering (ISMA), Leuven, Belgium, 2012, pp. 3501–3514.
[104] P. Sjövall, T. Abrahamsson, Substructure system identification from coupled system test data, Mech. Syst. Signal Process. 22 (1) (2008) 15–33, http://dx.doi.org/10.1016/j.ymssp.2007.06.003.
[105] W. D'Ambrogio, A. Fregolent, The role of interface DoFs in decoupling of substructures based on the dual domain decomposition, Mech. Syst. Signal Process. 24 (7) (2010) 2035–2048, http://dx.doi.org/10.1016/j.ymssp.2010.05.007.
[106] S. Voormeeren, D. Rixen, A family of substructure decoupling techniques based on a dual assembly approach, Mech. Syst. Signal Process. 27 (18) (2012) 379, http://dx.doi.org/10.1016/j.ymssp.2011.07.028.
[107] A.S. Elliott, Characterisation of structure borne sound sources in-situ (Ph.D. thesis), University of Salford, 2009.
[108] A.S. Elliott, A.T. Moorhouse, T. Huntley, S. Tate, In-situ source path contribution analysis of structure borne road noise, J. Sound Vib. 332 (24) (2013) 6276–6295, http://dx.doi.org/10.1016/j.jsv.2013.05.031.
[109] M.B. Madsen, Electrical power assisted steering—dynamic source strength characteristic and vehicle NVH prediction (Master's thesis), University of Southern Denmark, 2014.
[110] M.V. van der Seijs, E.A. Pasma, D. de Klerk, D.J. Rixen, A comparison of two component TPA approaches for steering gear noise prediction, In: Proceedings of the XXXIII International Modal Analysis Conference (IMAC), Orlando, FL, Society for Experimental Mechanics, Bethel, CT, 2015.
[111] M. Sturm, A.T. Moorhouse, T. Alber, F.F. Li, Force reconstruction using an adaptive algorithm in time domain, In: Proceedings of the International Conference on Noise and Vibration Engineering (ISMA), Leuven, Belgium, 2012, pp. 17–19.

[112] M. Sturm, A.T. Moorhouse, W. Kropp, T. Alber, Robust calculation of simultaneous multi-channel blocked force signatures from measurements made in-situ using an adaptive algorithm in time domain, In: Proceedings of the XX International Congress on Sound and Vibration (ICSV), Bangkok, Thailand, vol. 2, 2013, pp. 1610–1617.
[113] M.H.A. Janssens, J.W. Verheij, T. Loyau, Experimental example of the pseudo-forces method used in characterisation of a structure-borne sound source, Appl. Acoust. 63 (1) (2002) 9–34, http://dx.doi.org/10.1016/S0003-682X(01)00023-8.
[114] W. Weijtjens, G. De Sitter, C. Devriendt, P. Guillaume, Operational modal parameter estimation of mimo systems using transmissibility functions, Automatica 50 (2) (2014) 559–564, http://dx.doi.org/10.1016/j.automatica.2013.11.021.
[115] N.B. Roozen, Q. Leclère, On the use of artificial excitation in operational transfer path analysis, Appl. Acoust. 74 (10) (2013) 1167–1174, http://dx.doi.org/10.1016/j.apacoust.2013.04.011.
[116] Q. Leclère, N.B. Roozen, C. Sandier, Experimental estimation of transmissibility matrices, In: Proceedings of the International Conference on Noise and Vibration Engineering (ISMA), Leuven, Belgium, 2012.
[117] P. Gajdatsy, K. Janssens, L. Gielen, P. Mas, H. Van der Auweraer, Critical assessment of operational path analysis: effect of neglected paths, In: Proceedings of the XV International Congress on Sound and Vibration (ICSV), Daejeon, Korea, 2008, pp. 1090–1097.
[118] P. Gajdatsy, K. Janssens, L. Gielen, P. Mas, H. van der Auweraer, Critical assessment of operational path analysis: effect of coupling between path inputs, J. Acoust. Soc. Am. 123 (5) (2008) 3876, http://dx.doi.org/10.1121/1.2935777.
[119] J. Putner, H. Fastl, M. Lohrmann, A. Kaltenhauser, F. Ullrich, Operational transfer path analysis predicting contributions to the vehicle interior noise for different excitations from the same sound source, In: InterNoise12, New York City, NY, Number 3 in INTER-NOISE and NOISE-CON Congress and Conference Proceedings, 2012, pp. 2336–2347.
[120] D. de Klerk, M. Lohrmann, M. Quickert, W. Foken, Application of Operational Transfer Path Analysis on a Classic Car, 2009, DAGA, Rotterdam.
[121] J. Putner, M. Lohrmann, H. Fastl, Contribution analysis of vehicle exterior noise with operational transfer path analysis, J. Acoust. Soc. Am. 133 (5) (2013) 3323, http://dx.doi.org/10.1121/1.4805558.
[122] ISO Technical Committee 43/Subcommittee 1/Workgroup 22 (ISO/TC43/SC1/WG22), Measurement of Noise Emitted by Accelerating Road Vehicles—Engineering Method—Part 1: M and N Categories, ISO 362-1, International Standards Organisation, 2015.
[123] M. Vorländer, P. Dietrich, Transfer path analysis and synthesis for auralization, In: 39th Congreso Espanol de Acústica 2008, Coimbra, Portugal, 2008.
[124] K. Janssens, P. Mas, P. Gajdatsy, L. Gielen, H. Van der Auweraer, A novel path contribution analysis method for test-based NVH troubleshooting, In: Proceedings of the International Conference on Noise and Vibration Engineering (ISMA), Leuven, Belgium, 2008, pp. 3673–3683.
[125] K. Janssens, P. Gajdatsy, L. Gielen, P. Mas, L. Britte, W. Desmet, H. van der Auweraer, OPAX: a new transfer path analysis method based on parametric load models, Mech. Syst. Signal Process. 25 (2011) 1321–1338, http://dx.doi.org/10.1016/j.ymssp.2010.10.014.
[126] A. Blakeborough, M.S. Williams, A. Darby, D.M. Williams, The development of real-time substructure testing, Philos. Trans. R. Soc. A—Math. Phys. Eng. Sci. 359 (2001) 1869.
[127] V. Saouma, M. Sivaselvan (Eds.), Hybrid Simulation: Theory, Implementation and Applications, Taylor & Francis, 2008.
[128] T. Jungblut, S. Wolter, M. Matthias, H. Hanselka, Using numerical models to complement experimental setups by means of active control of mobility, Appl. Mech. Mater. 70 (2011) 357–362.
[129] D. Berckmans, P. Kindt, P. Sas, W. Desmet, Evaluation of substitution monopole models for tire noise sound synthesis, Mech. Syst. Signal Process. 24 (1) (2010) 240–255, http://dx.doi.org/10.1016/j.ymssp.2009.06.005.
[130] D. Berckmans, B. Pluymers, P. Sas, W. Desmet, Numerical comparison of different equivalent source models and source quantification techniques for use in sound synthesis systems, Acta Acust. United Acust. 97 (1) (2011) 138–147, http://dx.doi.org/10.3813/AAA.918394.
[131] K. Wyckaert, F. Augusztinovicz, P. Sas, Vibro-acoustical modal analysis: reciprocity, model symmetry, and model validity, J. Acoust. Soc. Am. 100 (5) (1996) 3172–3181, http://dx.doi.org/10.1121/1.417127.
[132] H.-E. de Bree, P. Leussink, T. Korthorst, H. Jansen, T.S. Lammerink, M. Elwenspoek, The μ-flown: a novel device for measuring acoustic flows, Sens. Actuat. A: Phys. 54 (1) (1996) 552–557, http://dx.doi.org/10.1016/S0924-4247(97)80013-1.
[133] H.-E. de Bree, An overview of microflown technologies, Acta Acust. United Acust. 89 (1) (2003) 163–172.
[134] D. Fernandez Comesaña, K. Holland, J. Wind, H.E. de Bree, Comparison of inverse methods and particle velocity based techniques for transfer path analysis, In: Acoustics 2012, 2012.
[135] P.A. Nelson, S.-H. Yoon, Estimation of acoustic source strength by inverse methods: Part I: conditioning of the inverse problem, J. Sound Vib. 233 (4) (2000) 639–664, http://dx.doi.org/10.1006/jsvi.1999.2837.
[136] S.-H. Yoon, P.A. Nelson, Estimation of acoustic source strength by inverse methods: Part II: experimental investigation of methods for choosing regularization parameters, J. Sound Vib. 233 (4) (2000) 665–701, http://dx.doi.org/10.1006/jsvi.2000.2836.
[137] J.D. Maynard, E.G. Williams, Y. Lee, Nearfield acoustic holography: I. Theory of generalized holography and the development of nah, J. Acoust. Soc. Am. 78 (4) (1985) 1395–1413, http://dx.doi.org/10.1121/1.392911.
[138] E.G. Williams, Regularization methods for near-field acoustical holography, J. Acoust. Soc. Am. 110 (4) (2001) 1976–1988, http://dx.doi.org/10.1121/1.1404381.
[139] I. Lopez Arteaga, R. Scholte, H. Nijmeijer, Improved source reconstruction in Fourier-based near-field acoustic holography applied to small apertures, Mech. Syst. Signal Process. 32 (2012) 359–373, http://dx.doi.org/10.1016/j.ymssp.2012.06.002.
[140] Y.I. Bobrovnitskii, G. Pavic, Modelling and characterization of airborne noise sources, J. Sound Vib. 261 (3) (2003) 527–555, http://dx.doi.org/10.1016/S0022-460X(02)00981-1.
[141] A.T. Moorhouse, G. Seiffert, Characterisation of an airborne sound source for use in a virtual acoustic prototype, J. Sound Vib. 296 (1–2) (2006) 334–352, http://dx.doi.org/10.1016/j.jsv.2006.03.017.
[142] G. Pavić, N. Totaro, Noise source characterisation using patch impedance technique, J. Acoust. Soc. Am. 123 (5) (2008) 3310, http://dx.doi.org/10.1121/1.2933750.
[143] B. Petersson, On the use of giant magnetostrictive devices for moment excitation, J. Sound Vib. 116 (1) (1987) 191–194, http://dx.doi.org/10.1016/S0022-460X(87)81332-9.
[144] M. Bello, A. Sestieri, W. D'Ambrogio, F. La Gala, Development of a rotation transducer based on bimorph PZTs, Mech. Syst. Signal Process. 17 (5) (2003) 1069–1081, http://dx.doi.org/10.1006/mssp.2003.1607.
[145] J. Liu, M. Li, L. Qin, J. Liu, Principle research on a single mass piezoelectric six-degrees-of-freedom accelerometer, Sensors 13 (8) (2013) 10844–10855, http://dx.doi.org/10.3390/s130810844.
[146] M.L.M. Duarte, D.J. Ewins, Rotational degrees of freedom for structural coupling analysis via finite-difference technique with residual compensation, Mech. Syst. Signal Process. 14 (2) (2000) 205–227, http://dx.doi.org/10.1006/mssp.1999.1241.
[147] L. Bregant, M. Sandersons, Rotational degrees of freedom: an historical overview on techniques and methods, In: Proceedings of the International Conference on Noise and Vibration Engineering (ISMA), Leuven, Belgium, 2000, pp. 973–980.
[148] M.A. Sanderson, C.R. Fredö, Direct measurement of moment mobility: Part I: a theoretical study, J. Sound Vib. 179 (4) (1995) 669–684, http://dx.doi.org/10.1006/jsvi.1995.0043.
[149] A.S. Elliott, A.T. Moorhouse, G. Pavić, Moment excitation and the measurement of moment mobilities, J. Sound Vib. 331 (11) (2012) 2499–2519, http://dx.doi.org/10.1016/j.jsv.2012.01.022.
[150] D. de Klerk, D. Rixen, S. Voormeeren, F. Pasteuning, Solving the RDoF problem in experimental dynamic substructuring, In: Proceedings of the XXVI International Modal Analysis Conference (IMAC), Orlando, FL, Society for Experimental Mechanics, Bethel, CT, 2008.
[151] S. Helderweirt, H. Van der Auweraer, P. Mas, L. Bregant, D. Casagrande, Application of accelerometer-based rotational degree of freedom measurements for engine subframe modelling, In: Proceedings of the XIX International Modal Analysis Conference (IMAC), St. Louis, MO, vol. 2, Society for Experimental Mechanics, Bethel, CT, 2001, pp. 1298–1304.

[152] M.V. van der Seijs, D.D. van den Bosch, D.J. Rixen, D. de Klerk, An improved methodology for the virtual point transformation of measured frequency response functions in dynamic substructuring, In: M. Papadrakakis V. Papadopoulos, V. Plevris (Eds.), 4th ECCOMAS Thematic Conference on Computational Methods in Structural Dynamics and Earthquake Engineering (COMPDYN), Kos Island, Greece, 2013, pp. 4334–4347. http://dx.doi.org/10.13140/RG.2.1.2715.3126.
[153] M.V. van der Seijs, D. de Klerk, D.J. Rixen, S. Rahimi, Validation of current state frequency based substructuring technology for the characterisation of steering gear—vehicle interaction, In: Topics in Experimental Dynamic Substructuring, vol. 2, Proceedings of the 31st IMAC, A Conference on Structural Dynamics, Springer, New York, 2013, pp. 253–266 (Chapter 20), http://dx.doi.org/10.1007/978-1-4614-6540-9_20.
[154] J.C. O'Callahan, P. Avitabile, R. Riemer, System equivalent reduction expansion process (SEREP), In: Proceedings of the VII International Modal Analysis Conference (IMAC), Boston, MA, vol. 1, Society for Experimental Mechanics, Bethel, CT, 1989, pp. 29–37.
[155] M. Allen, R. Mayes, E. Bergman, Experimental modal substructuring to couple and uncouple substructures with flexible fixtures and multi-point connections, J. Sound Vib. 329 (23) (2010) 4891–4906, http://dx.doi.org/10.1016/j.jsv.2010.06.007.
[156] R. Mayes, Tutorial on experimental dynamic substructuring using the transmission simulator method, In: Topics in Experimental Dynamics Substructuring and Wind Turbine Dynamics, vol. 2, Proceedings of the 30th IMAC, A Conference on Structural Dynamics, 2012, Springer, 2012, pp. 1–9, http://dx.doi.org/10.1007/978-1-4614-2422-2_1.
[157] W.D. Ambrogio, A. Fregolent, Inverse dynamic substructuring using the direct hybrid assembly in the frequency domain, Mech. Syst. Signal Process. 45 (2) (2014) 360–377, http://dx.doi.org/10.1016/j.ymssp.2013.11.007.
[158] Y.-P. Xiong, J. Xing, W. Price, A power flow mode theory based on a system's damping distribution and power flow design approaches, Proc. R. Soc. A: Math. Phys. Eng. Sci. 461 (2063) (2005) 3381–3411, http://dx.doi.org/10.1098/rspa.2005.1540.
[159] T. Weisser, L. Gonidou, E. Foltête, N. Bouhaddi, Optimization of substructure dynamic interface forces by an energetic approach, in: Structural Dynamics, vol. 3, Proceedings of the 28th IMAC, A Conference on Structural Dynamics, 2010, Springer, New York, 2011, pp. 801–809, http://dx.doi.org/10.1007/978-1-4419-9834-7_70.
[160] T. Weisser, E. Foltête, N. Bouhaddi, L.-O. Gonidou, A power flow mode approach dedicated to structural interface dynamic characterization, J. Sound Vib. 334 (2015) 202–218, http://dx.doi.org/10.1016/j.jsv.2014.09.012.
[161] M. Vorländer, Auralization: Fundamentals of Acoustics, Modelling, Simulation, Algorithms and Acoustic Virtual Reality, 1st ed., Springer-Verlag, Berlin, Heidelberg, 2007, http://dx.doi.org/10.1007/978-3-540-48830-9.
[162] D.J. Rixen, P.L.C. van der Valk, An Impulse Based Substructuring approach for impact analysis and load case simulations, J. Sound Vib. 332 (26) (2013) 7174–7190, http://dx.doi.org/10.1016/j.jsv.2013.08.004.
[163] P.L.C. Van der Valk, D.J. Rixen, Impulse based substructuring for coupling offshore structures and wind turbines in aero-elastic simulations, In: Proceedings of 53rd AIAA/ASME/ASCE/AHS/ASC Structures, Structural Dynamics and Materials Conference, Honolulu, Hawaii, American Institute of Aeronautics and Astronautics, 2012, pp. 23–26, http://dx.doi.org/10.2514/6.2012-1415.
[164] J. Yoshida, H. Ishihara, Method for the separation of vehicle interior noise contributions using only response signals, J. Syst. Des. Dyn. 7 (4) (2013) 416–427, http://dx.doi.org/10.1299/jsdd.7.416.